DURBAN UNIVERSITY OF TECHNOLOGY
INYUVESI YASETHEKWINI YEZOBUCHWEPHESHE

Coordinated Control of Conventional Power Sources and Plug-in Hybrid Electric Vehicles for a Hybrid Power System

By

Mohammed Ozayr Abdul Kader

Student Number: 21506129

Submitted in fulfilment of the requirements of the degree of Master of Engineering in Electrical Engineering in the Department of Electrical Power Engineering, Faculty of Engineering and the Built Environment

July 2022

Supervisor: Dr Kayode T Akindeji
Co-Supervisor: Dr Gulshan Sharma

ABSTRACT

Globally, the requirement for renewable and clean energy technologies is becoming vastly popular. With the high implementation of solar and wind energy systems, together with plug-in hybrid electric vehicle (PHEV) aggregators, energy costs can be minimised, greenhouse gas emissions decrease, and overall maintenance becomes reduced. The constant increase of load demand is becoming a challenge for the current power systems, with difficulties including stability concerns and excessive regulations by the government. Due to irradiance and wind speed fluctuations, the solar and wind energy system's non-linearity affects the existing power system stability. The growth of the electric vehicle industry has also shed new light on potential auxiliary services that can be provided, as and when required, to the power system. Hence, this research examines the potential control strategies that are required to maintain the system in steady-state conditions after disturbances that occur with higher penetration of renewable energy systems (RESs) and PHEVs. The case study models a isolated two-area thermal type power system that is interconnected through an AC tie-line. Three scenarios are modelled, simulated and analysed. The first scenario models a isolated thermal power system with PHEVs with two areas which utilises a fractional order proportional integral derivative (FOPID) controller in each area. The resulting model is analysed to see the effects of PHEVs coupled with FOPID on the power system. The second scenario models a isolated two-area thermal power system with RES and utilises a fuzzy type-2 (FT2) FOPID controller in each area. The RES penetration is tested for its non-linearity effect on the isolated power system, and the error is reduced by an advanced controller that uses artificial intelligence techniques. The third scenario is modelled as an isolated two-area thermal power system with PHEVs and RES coupled with neural network predictive controller (NNPC) in each area. The three scenarios are simulated in MATLAB/Simulink with results displayed graphically and numerically. The results show that the integration of PHEVs for load and/or storage in the multi-area power system, and the proposed control methods for each scenario, have the best dynamic response with the least error, no oscillations and the fastest response to steady state condition.

DECLARATION

I declare that this dissertation is my own work. All sources that I have used and quoted have been referenced. This work has not been submitted to any other universities for any other degree or examination.

This research was duly supervised by Dr Kayode Timothy Akindeji at the Durban University of Technology, and co-supervised by Dr Gulshan Sharma at the University of Johannesburg.

Submitted by:

…… 09 November 2022

Mohammed Ozayr Abdul Kader **Date**

Durban University of Technology

Department of Electrical Power Engineering

Student Number: 21506129

Approved for Final Submission by:

…… 09 November 2022

Supervisor: Dr Kayode T Akindeji **Date**

Durban University of Technology

Department of Electrical Power Engineering

…… 09 November 2022

Co-Supervisor: Dr Gulshan Sharma **Date**

University of Johannesburg

Department of Electrical Engineering Technology

PUBLICATION

The following publications emanated from this research investigation and form part and/or include research presented in this dissertation.

1. M. O. A. Kader, K. T. Akindeji, and G. Sharma, “A Novel Solution for Solving the Frequency Regulation Problem of Renewable Interlinked Power System Using Fusion of AI,” Energies, vol. 15, no. 9, p. 3376, May 2022, doi: 10.3390/en15093376.

2. M. O. A. Kader, K. T. Akindeji, and G. Sharma, "Application of PHEVs Influence on Frequency Regulation of a Two Area Power System," in 2022 10th International Conference on Smart Grid (icSmartGrid), 27-29 June 2022, pp. 23-28, doi: 10.1109/icSmartGrid55722.2022.9848535.

3. Mohammed Ozayr Abdul Kader, Kayode Timothy Akindeji and Gulshan Sharma, “Integration of PHEVs and Renewable Energy Systems in the Power System utilizing AI Neural Network Predictive Controller", Springer Nature. (Accepted, awaiting publication)

DEDICATION

This research and motivation are dedicated to my parents who have guided and educated me from the very first day. Most importantly, the compassion, almighty and mercy of God has allowed me to complete this research in perfect health throughout the Covid-19 pandemic.

ACKNOWLEDGEMENTS

"*The first step in knowledge is to listen, then to be quiet and attentive, then to preserve it, then to put it into practice and then to spread it.*"

- Sufyan ibn Uyaynah

Sincerest thanks to Dr Kayode T Akindeji and Dr Gulshan Sharma for their immense support and expert advice on this research. Your publications and thoughtfulness are very inspiring.

To my family, I appreciate all the support. See you soon at graduation!

TABLE OF CONTENTS

LIST OF FIGURES

LIST OF TABLES

LIST OF ACRONYMS

ACE	Area control error
RES	Renewable energy system
AC	Alternating current
DC	Direct current
AI	Artificial intelligence
DFIG	Doubly-fed induction generator
EV	Electric Vehicles
PHEV	Plug-in hybrid electric vehicle
GRC	Generator rate constraints
GDB	Governor dead-band
MPPT	Maximum power point tracking
LFC	Load frequency control
NNPC	Neural network predictive controller
CO_2	Carbon dioxide
SOC	State of charge
PID	Proportional integral derivative
FOPID	Fractional order PID
FL	Fuzzy logic
FT1	Fuzzy type-1
FT2	Fuzzy type-2
PV	Photovoltaic
PGF	Panel generation factor
NT	Nie-Tan method
SPWM	Pulse width modulation inverter
ITAE	Integral of time absolute error
COP26	UN Climate Change Conference UK 2021
PFC	Primary Frequency Control
CV	Constant Voltage
CC	Constant Current

PSO	Particle Swarm Optimisation
FIS	Fuzzy Inference System
IGBT	Insulated-Gate Bipolar Transistor
RODP	Reverse Osmosis Desalination Plant
HESS	Hybrid Energy Storage Systems
ITAE	Integral of time absolute error

1. INTRODUCTION

1.1 Background

As the global paradigm shifts in the electrical power industry amidst the 4th Industrial Revolution, clean renewable energy is becoming a more desirable way to produce power to protect the environment by reducing CO_2 emissions and the consumption of fossil fuels. The present challenge is how to increase the penetration of RESs and PHEV into conventional distribution networks without influencing the security, reliability and stability of the complete power system. The inclusion of clean energy sources would help reduce carbon tax and other penalties that electrical utility companies are charged with. These systems are also cost-effective in certain areas where clean energy is being produced.

Currently, South Africa's power utility, Eskom, cannot expand its generation capacity for thermal generation stations at a rapid rate due to the Department of Environmental Affairs' restriction on emitting CO_2 into the atmosphere. They are also faced with the increasing cost of fossil fuels such as gas and coal.

For generation reserve capacity, where maintenance and breakdowns occur, diesel fuel is required for backup. However, this fuel is limited and can only last a certain amount of time before being completely depleted. This contributes to load shedding roll-outs across South Africa that negatively impact the economy. Therefore, alternative energy sources are required to assist in this regard.

The bulk of power produced in South Africa is from coal, which is the highest from other power generation. While solar and wind power are becoming desirable in the current era as seen in Figure 1.1 below. The majority of South Africa's renewable energy power comes from Solar mainly within the Northern Cape and Wind within the Eastern Cape. The reason for this is due to the high output level of power these regions provide which is irradiance

and wind speed levels. The other province also generate power from hydro generation where the water flow is at a high level and has acceptable efficiencies.

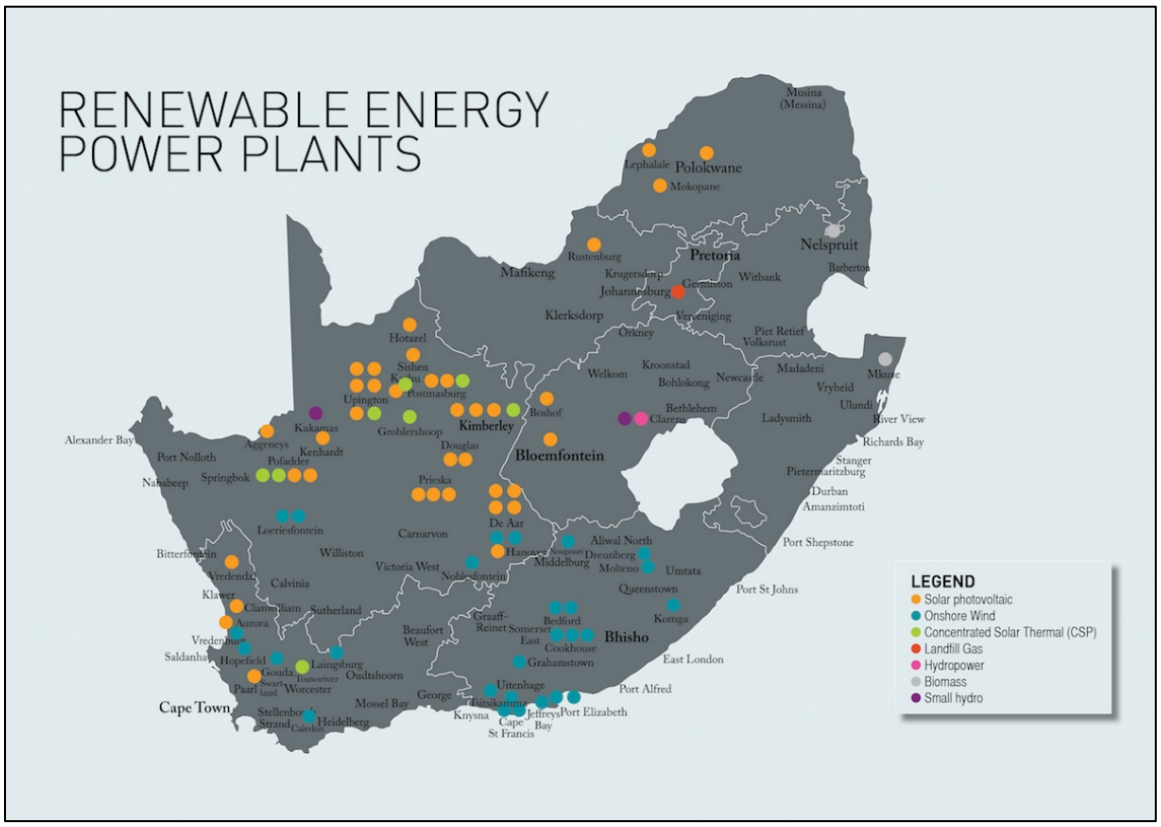

Figure 1.1: South Africa's Renewable Energy Power Plant [1]

Coal generation is around 69% of the total generation in South Africa and has only 1479 MW for solar, and 2096 for wind energy as seen in Figure 1.2. This makes renewable energy a high priority for the reduction of CO2 emissions within South Africa. Renewable energy power plants currently sit at 11% to 12%, with the intention of growing to 30% by 2030 [1]. As the injection of renewable energy increases, coal-powered fire stations will gradually decrease and become decommissioned. A sudden increase in renewable energy will result in a shock to the economic system of fossil fuel and related suppliers of coal-burning power stations. Therefore, a gradual increase in RESs is required.

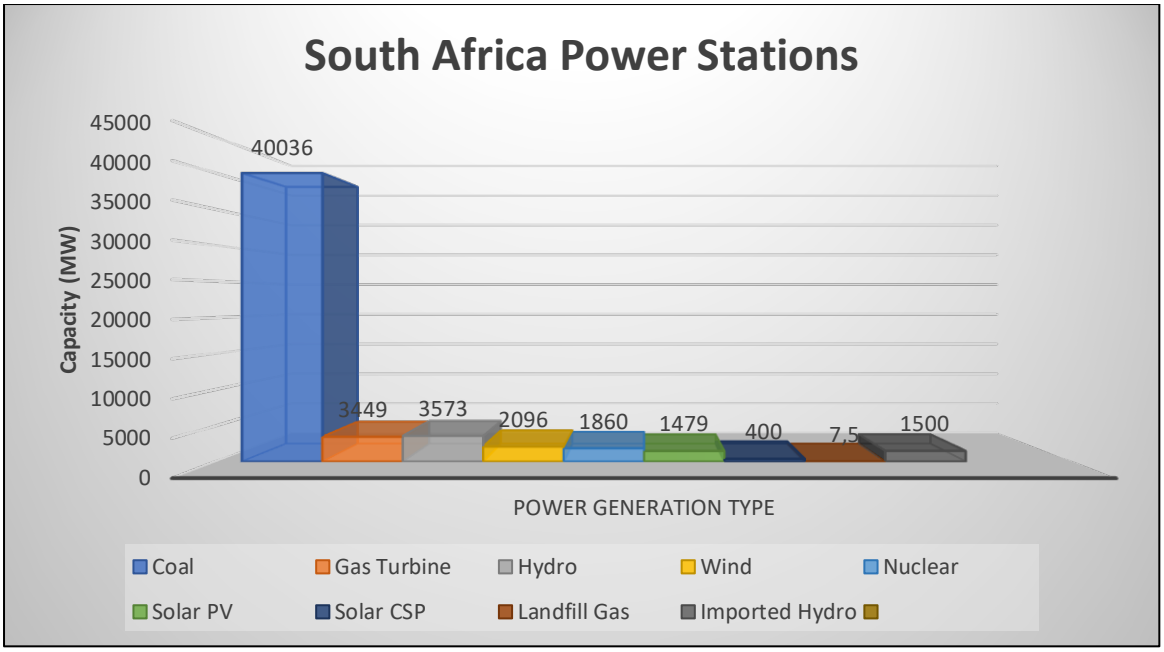

Figure 1.2: South Africa's power system capacities [2].

The inclusion of RES in the power system contribute to multiple frequency disturbances that disrupt the stability of the system. Overload of the microgrid occurs from PHEVs irregular charging patterns. To reduce the above-mentioned factors, various types of coordinated control methods are required.

In this research, FOPID FT2 control is used for frequency control which has the advantages of reducing overshoot, improving system response speed, and accelerating system stability time. The control effects are better with this controller compared to others. An optimisation technique by using NNPC will help improve the dynamic response.

For load coordination of PHEVs, charging strategies and energy management are required to reduce the voltage overload. This could create stress and cause serious damage to residential loads when multiple residents use PHEVs at the same time. Therefore, PHEV aggregators are used to balance out energy consumption to protect distribution transformers and the microgrid when charging and discharging PHEVs. PHEVs can also act as dump loads and storage banks which assist the power utility, as and when required, to prevent load shedding and its resultant economic losses and downtime.

1.2 Research Motivation

Producing clean energy is very important and has become very challenging. The move towards solar and wind power was increasing throughout the world. With climate summits and conferences calling for changes in the production of energy around the world, the push towards renewable energy has become a race to be carbon-free by 2050 [3]. Countries have already announced their milestones in percentages for 10-year increments to become clean energy producers. The goals of leading countries have encouraged the rest of the world into following this trend.

While this is good for one part of the transformation, there are technical complications that accompany it. Solar and wind energy sources are highly non-linear and variable, - in other words, solar irradiance from the sun and wind speeds cannot be predicted or controlled. Only predictive analysis can be used in this regard. This contributes to load and frequency variations leading to the tripping of power stations or severe damage to the equipment. Frequency load control methods are required with optimisation techniques from artificial intelligence or predictive software to stabilise the system.

South Africa, with her vast growing economy, has gradually affected the maintenance of load demands in areas. Some of the power stations are still being built in order to reach the full capacity, as envisioned. While the remaining turbine generators go online, the growth of the country is increasing at a higher rate than the expansion of the supply of power. With the addition of degrading and older power station equipment, keeping up with the supply has become a real challenge. Load shedding has become frequent, causing disruption to economic activities, damage to equipment and a loss of millions of rands in revenue.

1.3 Problem Statement

PHEVs are a new entrant into the power system networks, serving as load or storage, thereby altering the normal operation of the network. The following problems and issues to be addressed are:

1. PHEVs are emerging electrical components being integrated into power system networks, therefore, there is need for preliminary research and investigation to analyse their performance within the existing electrical grid;
2. Most countries have set milestones to be carbon-free to address global warming challenges by generating clean energy using renewable energy sources. However, without appropriate control mechanisms, a high penetration of RES will result in power system instability; and
3. The variable load patterns of consumer PHEVs and RESs make the system highly non-linear at different times of the day due to intermittent weather conditions. As such, there is a need for coordinated control of the resulting hybrid power system to secure its stability and reliability.

1.4 Research Aim and Objectives

The research aims to model an interconnected and isolated thermal power system with RES (solar and wind power) and PHEV aggregator with appropriate control for system stability.

The objectives of this research are:

1. To model an isolated two-area thermal power system with RES and PHEV aggregators on each area interconnected with an AC tie-line;
2. To design and optimise LFC methods to mitigate against high non-linearity through penetration of RES, tuning technique applications, and artificial intelligence methods;
3. To simulate the dynamic responses of the power system with multiple controller strategies and frequency/tie-line power stability without the inclusion of RES and PHEVs; and
4. To compare and contrast the performance and response of each proposed controller and make recommendations.

1.5 Research Methodology

The research methodology is as follows:

1. Conduct an extensive literature review pertaining to clean energy systems, control strategies, optimisation and usability;
2. An examination of the modelling with the inclusion of RES and PHEVs interconnected;
3. Develop the transfer functions for power systems and clean energy systems for initial analysis of the frequency control.;
4. Design control strategies such as PID and FOPID;
5. Optimise performance with artificial intelligence such as interval FT2 and NNPC;
6. Computational modelling of the interconnected system using MATLAB/Simulink;
7. Graphical simulation for the output results of the two areas and tie-line to be analysed; and
8. Evaluate the performances of the various controllers with a change in demand.

1.6 Dissertation Outline

The subsequent chapters of this dissertation are structured as:

1. Chapter 2 showcases a comprehensive literature review on topics relating to this research. A theoretical discussion provides insight into the requirement for renewable energy sources, clean energy and alternative ways to operate the present power systems;
2. Chapter 3 describes the modelling of thermal power systems and subsystems consisting of solar PV systems, wind power systems, and PHEV. Different control strategies and methodologies are also presented for a resolution on stability of the system improvement;
3. Chapter 4 presents a simulation results with graphical illustrations and numerical values for ease of interpretation, and comparison for the multiple configurations of power systems that are interconnected with sub-systems; and
4. Chapter 5 is the concluding chapter highlighting possible improvements to enhance the results and future research work.

2. LITERATURE REVIEW

2.1 Frequency Influence on Thermal Power Plants

The balance between load and demand is highly dependent on the power system frequency stability. Frequency stability has long-term and short-term stability that can provide a variety of influences for the power generation and loss of loads. To ensure that the power system is in a stable condition, the balance between supply and load demand is required.

The increase in load demand contributes to the decrease of the system frequency; while the decrease in load demand contributes to increasing of the system frequency. Frequency is regulated through a band of minimum and maximum limits to protect power system equipment.

System frequency is never stable, making it challenging for voltage and frequency to be within the stable parameters. The control system frequency of a thermal power plant usually has the generator speed varied, with the governor regulating this speed through constant monitoring. The generator speeds decrease with an increased load which contributes to decreased system frequency. The requirement for control is required to keep the system within steady-state conditions after some disturbance.

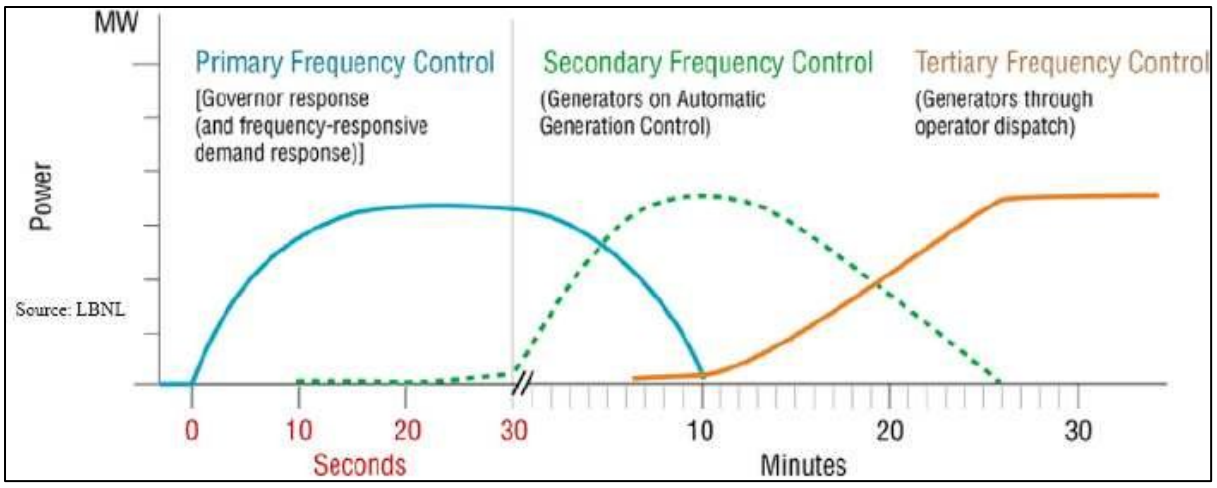

Figure 2.1: Types of Frequency Control [4]

The system has three frequency controls; primary, secondary and tertiary. The primary frequency control does not fully return the system frequency to its original condition, but assists with stabilisation. The generator's inertia is used to normalise the system frequency. Generator governors have a dead-band region within this control that will activate between this region [5]. Droop auxiliary is also made of use to return the frequency to its original condition.

The secondary frequency, which commonly is the automatic generation control (AGC), returns the system within the balanced region and assists the primary frequency control [6]. If the secondary frequency control cannot assist the system frequency to its normal state, a tertiary frequency control alters the power interchange, regulating load shedding/reduction and manages generator setpoints [7].

Frequency contributes to many demeriting factors, such as frequency regulation that is required to protect the blades of the turbine. Power transformers affect flux in the core due to frequency fluctuations, and set frequency used to manage motor speeds.

2.2 Renewable Energy Systems Integration

The depletion of fossil fuels and daily increases in pollutant emissions are of great importance, which is why countries are employing renewable energy solutions [8]. Germany is attempting to become fossil fuel-free by 2030, with the remainder of Europe aiming for 2050. The movement towards renewable energy has become the world's mission, eradicating fossil fuels that are negatively impacting the environment will possibly be depleted in the near future, and the challenge of procurement which decreases power capacity when not available at critical moments. At the latest COP26 climate summit, countries around the world committed to reducing carbon emissions over the next few years [9]. As the horizon of the year 2050 for clean energy approaches, the pressure to implement renewable energy is becoming very high.

With South Africa far behind other countries in renewable energy, implementing high-capacity clean energy remains a challenge. The increase in RESs is becoming very common due to the mitigation of carbon emissions and reduction of fossil fuels. However, by

increasing clean energy in the power grid, uncertainty is increased in the system. The systems that are mainly used include solar, wind and hydropower. These methods are highly sought-after but have negative effects, including increasing the system frequency disturbances and higher costs [10]. The balance between the interconnected systems is required to prevent power loss and disturbances that will bring more harm to the power grid.

RESs are known to affect power quality issues. For solar and wind power, the wind speeds and solar radiation vary, resulting in inconsistent generation to power electronic devices. The power electronics do provide has challenges with inrush currents, resonance phenomena and harmonic injection [11]. RESs also have voltage fluctuations and frequency deviations. Due to low synchronous power generators in the power network, which influences the rate of change of frequency, the penetration contributes to instability from its power electronics, such as inverters.

RESs cannot provide inertia naturally like synchronous generators which change according to demand. For instance, using doubly-fed induction generators, the active and reactive power flow is regulated on the rotor side. A constant DC link is managed by the converter on the grid side, which ensures the rotor side maintains the unity power factor. This wind-powered system doesn't affect the performance of wind speeds due to its arrangement, which assists the supply of power at grid frequency from the stator area. The rotor side manages the rated power by reducing losses which, in turn, reduces the cost. The reason for this is that the mechanical stresses of the wind turbine are decreased due to managing high wind speeds using the controlled operating point of the turbine [12].

Wind power is also becoming popular in China and other regions where good wind speeds are available. The improvement of wind turbine capacity and penetration of wind power into the power grid is increasing rapidly, curbing the uncertainty and output variance of these systems [13]. Inertia control is one of the proposed analyses for control in wind power systems [14].

Analysis of wind power variation with annual horizons are being undertaken to reveal a coefficient of variation and standard deviation of wind power ramping rate, so as to understand wind power fluctuations. This analysis will assist with control methods and investment reduction [15]. Control strategies, such as closed-loop proportional-integral load frequency controllers, are also utilised as a way to maintain the stability of current and voltage in the power system with the penetrator of clean energy systems [16].

Similar to solar power, the seasons also affect wind power systems due to the wind speeds which, in turn, requires statistics to be undertaken to assist with power outputs [17]. The transient stability control of wind turbines can be understood through formulated performance criteria to deduce the outcomes of stability in interconnected power systems [18]. Limiters are employed in the wind power system, such as maximum power point limiter and power smoothing, to enable operational stability. The energy yield can be increased by 6% through control structures [19].

DFIG wind-based energy schemes have been shown to assist with system stability after a fault has occurred, but rely on the type of control method option. One of the phenomena experienced by series-compensated wind power systems is sub-synchronous resonance. Dynamic reactive power reference signals at the point of common coupling are required to ensure that the reactive power supply is upheld [20, 21]. DFIG shares properties of inductive and synchronous generators which further contribute to the power system stability. Without interfering with voltage control, the damping of power variations in the power system can be improved through effective control. One of the control methods researchers use is diode rectifiers for wind power systems which contribute to stability error reduction while increasing output active power. With active and reactive power playing an important role, information gathered from scholars indicates that wind turbines, with varying wind speed over time, reduces voltage fluctuations [22-25]. The governors of thermal power units do not have the necessary measures to reduce frequency deviations because of their stagnant response and lack of control.

RESs fluctuations are removed due to the control systems that provide flat voltage on the DC link [26]. By imitating a conventional control framework with parallel synchronous generators, the distributed generation shares the load request without communication, which is the function of a droop control to control renewable energy integration into the grid. An improvement of this is the robust droop control which enhances accuracy and fluctuation reduction [27]. Controllers, such as virtual synchronous generator controllers, have many configurations. Their main function is to provide "virtual inertia" that slows down change of speed by providing the rotor swing equation [28, 29]. This assists in providing more usable energy while reducing costs. The systems are becoming more advanced with the increased involvement of solar power in the industry.

Using advanced algorithms such as particle swarm optimisation (PSO) for maximum power point tracking (MPPT) can assist in maximising the efficiency of clean energy generation [30]. Another method relating to solar power systems is IGBTs which assist with the distorted load currents through the coordinated control of unbalanced loads with high variation of irradiance [31]. The irradiance is known to be higher in spring and summer, which offer better conditions for irradiance harnessing. This contributes to the non-linearity of the variations of output power at different seasons [32]. The operational cost and maintenance are deemed important for feasibility studies, with the variation of irradiance across different seasons [33]. Solar PV has also known to assist with desalination plants - another renewable method of obtaining safe and clean water. The grid-connected solar PV was shown to assist the RODP in Sharjah greatly by reducing the cost of power by 70% and emissions of CO_2 by 78.8%. This is a great achievement and proof that solar power is one of the best alternative sources of clean energy [34].

PV-based solar incorporates an inverter within its system, which reduces system inertia and makes the system more susceptible to disturbances. While disturbances pose a problem to the power grid, the efficiency of wind and solar systems is very low, and they are proposed depending on the application to be used as a coupled generation system. Maximum power point tracking (MPPT) control for the renewable system is an effective way to maximise the low efficiency given while connected to the power grid [16, 32, 35-40]. This system

inertia was responsible, in conventional power systems, for suppressing the small frequency excursions in the wake of unexpected load alterations.

The cost of solar power is also reducing because of the mass usage of this technology, helping developing countries such as South Africa. Even though this is the case, it is still difficult to consider a rapid change that can affect other stakeholders such as coal distributors, system professionals, government-based entities, etc. The answer to this problem was to implement a gradual change to clean energy while decommissioning fossil fuels at a slower rate. This assists with the mitigation of non-linearity by introducing AI techniques, frequency controllers, and automatic voltage regulators for the smaller disturbances which are possible to control.

International funding from first-world countries is encouraging neighbouring countries to move towards renewable energy, since this is going to be the dominant generation of power worldwide [41]. This is necessary as the fossil fuel production and supply will moderately decrease, leaving behind countries that are still reliant on fossil fuel-powered stations.

2.3 Applications of Plug-in Hybrid Electric Vehicles in the Power Grid

With the current fuels prices for petrol and diesel rising due to disturbances in high-capacity distributors of crude oil, the promise of the implementation of electric vehicles is becoming more attractive. Governments also have concerns about air-polluting emissions that require the private and public sectors to contribute to air purification. The transportation sector contributes to 14 to 19% of greenhouse gas emissions [42, 43]. Even though the production of the combustion engine for vehicles has become more efficient in the release of CO_2, the increasing annual number of motorists on the road is keeping emissions in a constant state. PHEVs are currently becoming popular as we strive towards zero carbon emissions into the atmosphere. EVs are also known to provide an adequate, reliable supply of power through smart grid applications combined with RESs [44]. Therefore, PHEVs will assist in the transition to a low-carbon economy that will improve air quality, reduce noise levels,

lower traffic congestion, and improve the safety of roads through advanced monitoring systems.

The possibility of using PHEVs has become a major topic in the modern age where clean energy and the reduction of carbon footprints are required. The use of these vehicles in recent years has shown that they can assist with power system stability. With an increased number of electric vehicles being bought every year; the grid needs to be managed through coordinated control methods. PHEVs have double the benefits as they compensate for clean energy and have zero carbon emissions. This plays a major role in the production of electricity and lowering transportation costs [45].

The inclusion of the PHEV system needs to be integrated in a way to achieve the benefits of frequency stability. PHEVs can be utilised as a quick power source to support the frequency control loops for frequency response improvement of power systems and RES. PHEVs are an excellent option due to their fast-acting capability, distribution availability and slow discharge rate while in idle condition. To incorporate this, charging stations for electric vehicles are a critical component for allowing the smooth functioning of an electric vehicles (EVs) state-of-charge patterns [46-51]. Charging of PHEVs is also considered of high importance due to potential harmonics and stability issues [52]. Strategies of charging management are shown to reduce cost, especially when PHEVs are connected to the grid and help with two-way power flow auxiliary services that can potentially provide reimbursement [45].

The ancillary services of using PHEV are similar to battery systems that are capable of frequency support to the power grid. PHEV's owners can be remunerated for the auxiliary services they can provide to the power grid. These have been shown in [53] to have effective balancing properties for load and demand, with faster response times. However, there are uncertainties when bulk EVs are charging on the grid. Power management and SOC-based coordination are crucial for power at peak times and line loading. They are known to assist with shaving off additional power at peak load conditions which, in turn, increases efficiency while reducing cost [54], also shown in [55] to reduce the grid dependency.

While incorporating PHEVs, secondary control action plays a pivotal role in achieving high-speed restoration of the system frequency to steady-state conditions. The power generation areas are capable of exchanging power with the help of an AC tie-line, resulting in an interconnected network that is highly reliable and cost-effective - commonly referred to as control areas. It is, however, recommended that each generation area meet its demand for power while controlling the power exchange between tie-lines [32].

The LFC regulators are implemented in the power system to manage the frequency deviations. Their role is to link the electrically generated power with the present load to minimise or set the area control error (ACE) to zero value. LFC schemes based on optimal control provide the optimum performance by minimising the certain performance index. Extensive research was done on the LFC and many renewable-based power generation technologies capable of improving the LFC performance, such as wind and photovoltaic power for the LFC of an electrical energy system [56, 57].

The connection of PHEVs can affect the low voltage grid negatively, creating voltage instability [58]. The PHEVs can assist the grid when idle, and offer or remove additional energy through the vehicle-to-grid (V2G) concept. The management of the charging patterns of these vehicles is important for penetration into the grid, as this can affect transmission through the electrical grids and economic markets. Control strategy designs are required to manage energy performances by communicating between V2G [59]. Through optimisation using hybrid energy storage systems (HESS) and energy management strategies, the PHEV energy efficiency was shown to increase by 2.5% [60]. Using V2G system applications, the technology is known to assist with the reduction of equipment failure in the power grid and provide protection through peak load mitigation [61].

The high drivable range for PHEVs is a major advantage, especially on longer trips, as well as fuel-efficient backup combustion engines in case of difficulty in locating a charging station [62]. PHEVs are known to be more efficient than gasoline-powered vehicles by two-to-three times. However, it can be argued that the hybrid generation of power sources

required to charge these vehicles can also result in greenhouse gas emissions. This is when RESs are needed to counteract such challenges.

If a large fleet of PHEVs connects to the grid at once for charging, a large spike could occur which will overload the grid. Therefore, a centralised communication system, such as a charging station, is required to manage the electric vehicles. The centralised system, while connected to the electric vehicles, can also stabilise the load curve of the power grid by reducing the loss of energy [63]. It's also noted that charging electric vehicles at night can sync well with wind power outputs, while daytime charging syncs well with peak solar outputs. The connection between PHEVs and RESs appears to work well in the supply and demand of power.

While the cost of electrical vehicles is high at the moment, there's a possibility that the cost of lithium-ion batteries will reduce further if there's an increase in electric vehicle production. It was stated that almost 50% of the cost comes from the battery, which has a major impact on consumers who purchase these vehicles and contribute to clean energy usage. A study done indicates that the daily cost of energy, when linked with vehicle-to-home (V2H) technology, has great economic profitability potential [64].

The additional power required by the grid can be sold from PHEVs to offset energy bills or generate an income for consumers. For these benefits to become a reality, government policies have to cater to these changes, with adjustments to the market and social acceptability of fossil fuels [65].

2.4 Area Control Error through Optimised Frequency Controllers

The change of the indirect shape amount from the load frequency control strategy is known as area control error. The area control error monitors parameters through closed-loop vector feedback and restores systems to normal operating conditions through corrective actions for parameters. The area control error is generally installed in each area. Techniques that perform well against non-linear systems and multiple scenarios include artificial

intelligence, such as article bee colony, ant colony, particle swarm optimisation, neural networks, fuzzy logic systems and other optimisation algorithms. These optimised coordinated controllers assists with the reduction of operational costs [66].

One of the load frequency controllers, known as "PID controllers", are commonly used. Three constants are included in PID which are; proportional gain, integral gain and derivative gain. They can also be used as PD controllers or PI controllers, depending on the output results required [67]. PI controller has shown, in previous research, to have a significant disadvantage due to poor damping, thereby requiring refined-tuning formula to improve performance. The PI controller with optimisation - called particle swarm optimisation (PSO) - is used to obtain optimum values for the coefficients [68]. This optimisation comes from artificial intelligence strategies used by researchers for enhancing output results. The measurement of performance has commonly incorporated integral of time absolute error (ITAE) for minimising error used by researchers for its high accuracy in LFC [69].

An upgrade of the PID is the FOPID, with two more degrees of freedom used in load frequency control. PID controllers have the disadvantage of noise occurring in the derivative area of the equation. They are also linear and symmetric, which makes the performance of the controller vary. Therefore, the additional parameters for FOPID are input into the formula to help mitigate these [70]. This controller was seen to work on multi-area power systems successfully. FOPID has also been known to work well with uncertainty. FOPID is shown in [71] to provide positive effects with RESs, contributing to highly non-linear systems. FOPID has proven to be efficient in uncertain environments as have PHEVs with frequency enhancements which are rarely seen in two-area network research, therefore these components will be utilised in this paper for their benefits, presented in the literature [70, 72-75].

Further enhancement and optimisation such as AI techniques i.e., FL have been integrated and tested successfully for applications that require control. The control algorithm has shown to be highly effective and contributes to a significant performance increase regarding settling times, overshoots, and other performance criteria [56, 76-80]. This

controller can assist non-linear systems greatly, rather than the slower traditional controllers available. When combining the PID and fuzzy logic, the advantages increased when is better control available. A two-input fuzzy PID controller can be obtained by using a fuzzy PI or fuzzy PD controller. Depending on the output desired, the controller configuration is selected [81, 82].

An extension and advancement to conventional FL is the fuzzy type-2 which includes an NT type reduction process that converts type-2 to type-1 and then gets the final defuzzification result. The FT2 is much more suited to highly non-linear systems than to renewable interlinked power systems. FT2 has shown to have better performance than FT1 and PI controller methods in multi-area power systems. By adjusting or including an increased number of rules for the interference mechanism, the controller performance can be increased in fuzzy logic systems, according to some researchers. A high complex fuzzy logic system is the FT2 provides more computational iterations and greater results to uncertainty. The optimal gains and parameters of these controllers can be achieved through optimisations methods such as particle swarm optimisation, genetic algorithm, artificial bee colony, and others available [83]. This assists with achieving the best performance the controller can offer to the power system.

Another controller, known as the neural network using predictive technology, was known to predict simulation outputs of the power system and provide optimal responses with less error available. The neural network controller is also able to overcome drawbacks of limited real-time availability of data, and has operating conditions over a wide range dynamic performance that are highly suitable for load frequency control. The neural network with a recurrent link has a feedback connection which allows the network to generate time-varying patterns that can improve load frequency control in the power system through the optimal control design [84]. The NNPC controller uses a method called online training that runs iterations of the output which can be tuned [85]. The online learning training algorithm for NNPC under different types of fault conditions is highly effective and offers global stability to the power system. The dynamics are also captured more effectively [86]. An offline predictive controller can be incorporated to produce higher power outputs with fewer online

calculations, but this requires higher control actions through auxiliary equipment that can be costly [87].

Even if the system parameters have uncertainty involved, the neural network can retain the robustness of the system [88]. The superior neural network has also been compared with load frequency controllers (LFC), such as PI controllers, which resulted in better performance under varying load conditions and are suitable for renewable energy technologies [89]. Further enhancement of control strategies are required to assist with the gradual increase of the renewable energy included in the power system [71], therefore making the neural network is a good approach to obtaining stability.

Performance criterias are used to prove this by calculating the area of the control. One such method is used is Integral Time Absolute Error (ITAE) which can be tabulated to evaluate with ease of understanding [73, 90-92]. It is important that, if fluctuations occur, the system returns to its nominal value. In a two-area power system, the controllers are required in both areas to maintain the power interchange at scheduled values, as well as to minimise the frequency deviations for unexpected load alterations.

Multiple control methods can be utilised, depending on the power system reaction to disturbance that needs to be corrected. Depending on the structure and processes of the controller, the error can be reduced and/or eliminated.

2.5 Chapter Summary

In this chapter, the reasons for issues of the power grid are explained, with suggestions for potential sub-systems that could assist with additional energy and control. Since the effects of climate change are becoming more evident through adverse weather conditions, clean, renewable energies are the next sources for the generation of power - but these pose challenges with the integration into the current power system.

3. DESIGN AND METHODOLOGY

3.1 Design of an Isolated Thermal Power System with PHEVs and Application of Fractional Order PID Controller

3.1.1 Introduction

As the world moves towards a cleaner environment by reducing carbon emissions, clean energy is becoming more desirable with the usage of RESs, hydropower and electric vehicles. Directives from world bodies have obliged members to achieve 20% shares of energy from renewable energy sources in communities. With the major demand for energy in developing countries, alternative solutions are required to help reduce the current system instability, while moving towards a clean way of producing electricity. The maintenance needed to keep South Africa's 50Hz frequency regulation to the end-user is of the utmost importance. Therefore, the requirement of LFC becomes imperative for the regulation of frequency.

Currently, the concepts of reduced-order modelling and internal model control have been researched frequently. However, there are limitations in certain environments that require improvements. An LFC application is FOPID which offers more freedom, flexibility and dynamic responses than traditional PI and PID controllers in terms of non-linearities and uncertainties. These, in turn, enhance the stability of the power system. For this research the following will be covered:

1. Develop an isolated two-area thermal power system used for frequency stability studies utilising the first-order linear transfer function approach;
2. The isolated power system is thereafter injected with PHEVs on each area of the isolated thermal power plant and interconnected via an AC tie-line;
3. Multiple secondary controllers are designed with their relevant gain values such as PD, PI, PID and FOPID;
4. Manual tuning and system tuning are done to acquire the optimum value of gains for the controllers;

5. Step load alterations are done on the power systems for behavioural patterns;
6. Data is presented graphically for 1% load disturbance in area 1. Then graphical results for both area 1 and 2, with 1% and 2% respectively, are shown for confirmation of output results. ITAE performance criteria are tabulated for 1% load change.
7. Analysis of the results, compared with the various controllers under the same conditions, show the discovery of the research done by achieving steady state at the quickest time.

3.1.2 Isolated Power System Model

The tie-line for two isolated power systems is interconnected to allow two-way power flow between the two areas. This is represented in a simplified Figure 3.1 below. The model shown in Figure 3.2 displays the transfer functions with the inclusion of PHEVs.

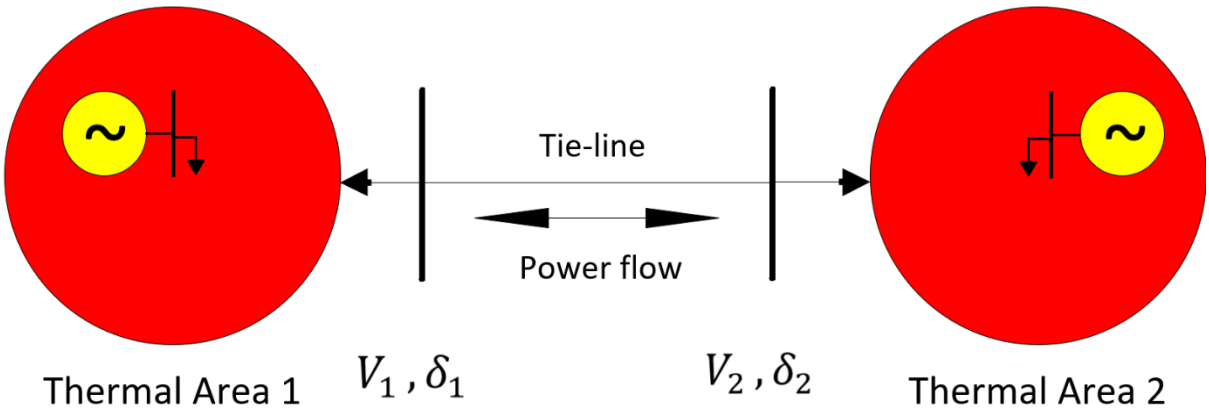

Figure 3.1: Two-area isolated power systems interconnected via tie-line.

The isolated two-area thermal power system is illustrated below, showing the basic process of the generation of power using the primary equipment for analysis purposes such as the governor, turbine and generator. The isolated power system is integrated with a PHEV aggregator in each area to assist the system with supply and load demand scenarios at various patterns during the day. An LFC of various configurations and types is used in each area to control uncertainties and disturbances from the system. These controllers are used to compare the performances and behaviour of frequency, which will bring the system back to steady-state conditions. In this research, the isolated power systems for each area are identical, with varying changes in power demands

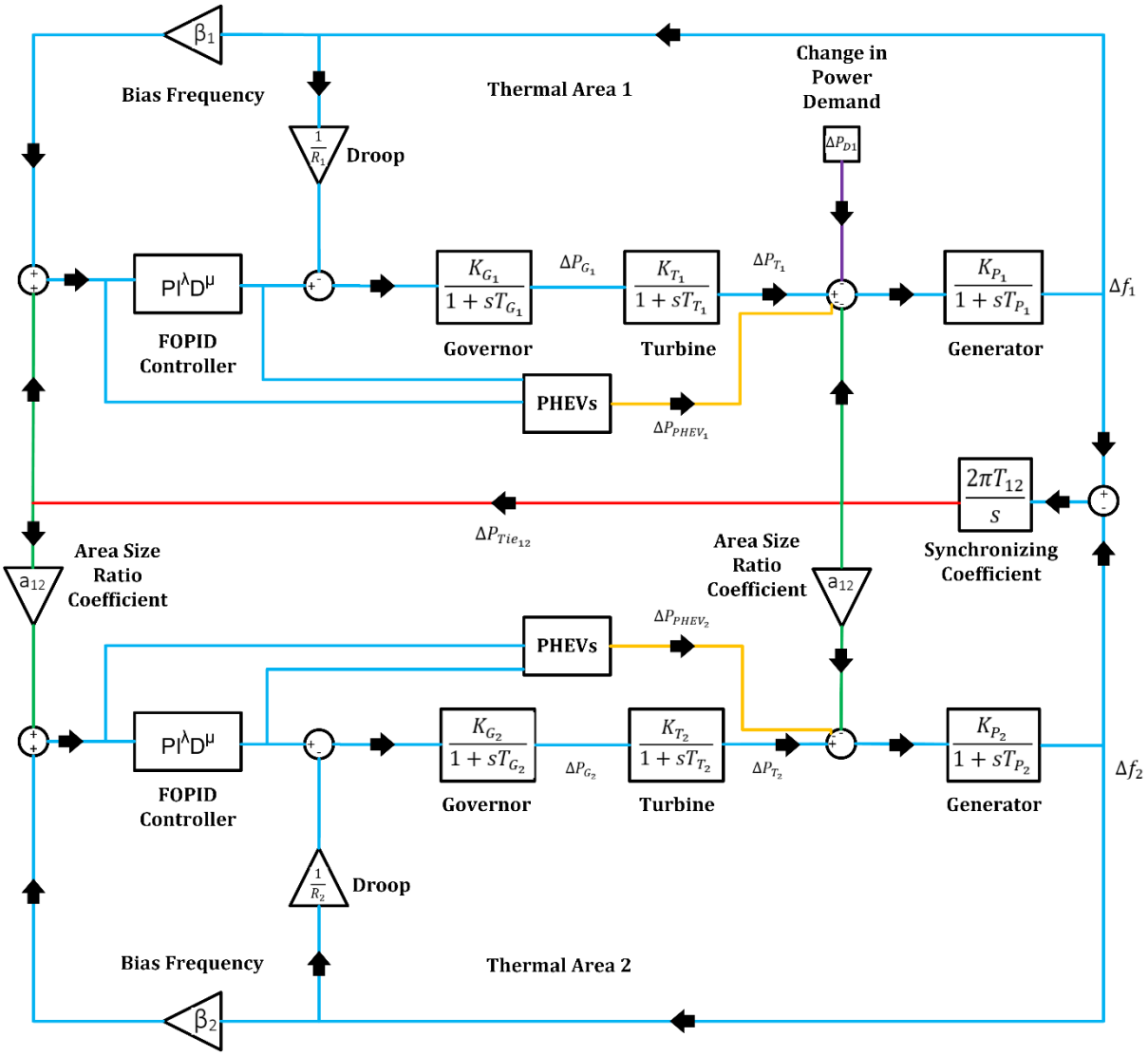

Figure 3.2: Two-area system model with PHEVs.

The control area consists of generators that maintain the relative power angles, either by increasing or decreasing their speed. The LFC maintains a turbine speed governing system for steady-state conditions due to load demand changes. This system of a steam turbine has four components which are:

1. Fly ball speed governor that senses the change in speed/frequency;
2. A hydraulic amplifier that has main piston and a pilot valve that opens or closes the steam valve against the pressure steam;
3. Linkage mechanism that provides movement to the control valve in proportion to change in speed and feedback from the steam valve movement; and
4. A speed changer which provides a steady state power output setting of the turbine.

The speed governing system model, and derivation of the transfer function, considers the system initially operating at steady-state, with the linkage mechanism unvarying, pilot valve closed, opened position of steam valve by a certain magnitude, and constant speed of turbine while the generator load is balanced due to turbine output power. A linear incremental model is determined using the conditions mentioned. By making assumptions about the behaviour of the turbine speed governing system, a Laplace transformation of the equations is generated. From here, the governor speed regulation, the speed governor gain, and the time constant of the speed governor are derived.

The steam turbine model considered is a non-reheat turbine which will consist of a single equivalent time constant for ease of analysis. The turbine time constant and gain can be seen in Table 3.1.

Table 3.1: System parameters for isolated thermal power system.

Parameters	**Values**
Governor time constant	0.4 sec
Turbine time constant	0.5 sec
Generator time constant	20 sec
Governor/turbine gain	1
Generator gain	100
Speed regulation	3
Area size ration coefficient	0.425
$2\pi T_{12}$	0.05

The generator load model is derived using the incremental turbine power output where generator losses are assumed to be negligible, the rate of change of kinetic energy in the generator rotor, and the rate of change of load due to frequency changes. The generator gain of the power system, and time constant, are thereafter derived. A two-area interconnected power system, the tie-line connects the two areas where power is transported in and out. The equation for tie-line power is:

$$P_{tie,12} = \frac{|V_1||V_2|}{X_{12}} \sin(\delta_1^o - \delta_2^o) \tag{1}$$

Where:

V_1 = Voltage magnitude in Area 1

V_2 = Voltage magnitude in Area 2

X_{12} = Net reactance of the tie line

δ_1^o = Power angle in Area 1 machine

δ_2^o = Power angle in Area 2 machine

By using the incremental changes of frequency and Laplace transformation, the synchronising coefficient equation is used as part of the simulation. The area control error is redefined as a linear combination of incremental frequency and tie-line power which is:

$$ACE = \Delta P_{tie}(s) + b_1 \Delta f_1(s) \quad (2)$$

Where:

ΔP_{tie} = Tie Line power

b_1 = Area frequency bias

Δf_1 = Frequency Change

Where frequency bias is included in equation (2), the determination of area size ratio coefficient is determined from the change of power tie-line in area 1 and area 2. The speed changer provides a frequency of 100% at full load, while at steady-state load frequency, characteristics between frequency and load for free governor operation show a linear relationship which is represented in the droop.

3.1.3 PHEV Aggregator Model

The PHEV aggregator behaves as a centralised communication centre between electric vehicles and the power grid. This system manages the charge and discharge of electric vehicles. The aggregator consists of a primary frequency control (PFC), LFC signal from area 1 or 2 controllers, and a battery charger model. The participation factor has also been included as part of the model due to considering PHEV's state of charge (SOC) which varies during the day. According to the PHEVs operating modes, the participation factor

K_i is used to determine the participation of each electric vehicle in the primary frequency control area. Depending on the state of charge, which changes from zero to one, the participation factor can change according to the usage during the day, which affects the PHEV's operating modes. The PHEV can operate in three modes; disconnected mode, charging mode, and idle mode. Parameters used for the purpose of this model were obtained from [45] and can be seen in Table 3.2.

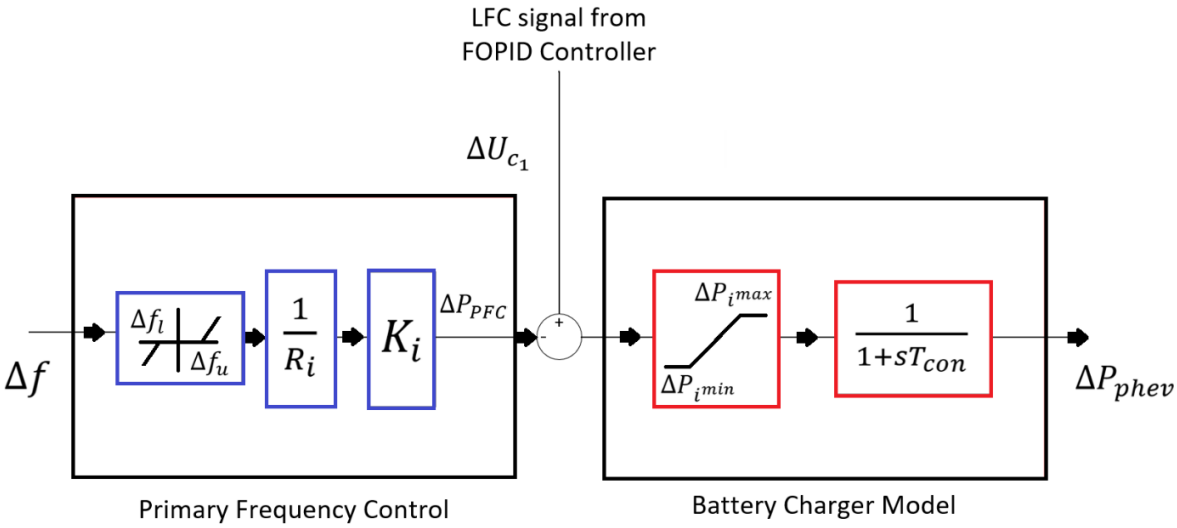

Figure 3.3: PHEVs aggregator model including average participation factor.

Table 3.2: System parameters for PHEV.

Parameters	**Values**
Dead Band	±10mHz
1/R	100
SOC_{av}	76%
K_{av}	0.9
$T_{conv,av}$	50ms
ΔI_{av}^{max}	10A
ΔI_{av}^{min}	-11A
$V_{d,av}$	391.2V

Components of the aggregator are explained for the requirement and operation of EV connected to the grid. The dead-band function is utilised by all generating units involving primary frequency control (PFC) with the upper Δf_u and lower Δf_l limits. This is used to avoid uninvited small frequency perturbations that may cause excessive wear and tear in the turbine, which, in turn, increases maintenance costs. The frequency droop coefficient R_i controls the output active power according to the input frequency deviations. This controls the increases in the PHEV power by ΔP_{PFC} for the frequency drop of Δf. PFC loop integrates participation factor k_i. The participation is determined by the PHEVs operating modes. This value, which varies from zero to one, is dependent on varying SOC. The average power for a PHEV is within the primary reserves of the upper limit ${\Delta P_i}^{max}$ and lower limit ${\Delta P_i}^{min}$. This represents the number of reserves which can be consumed over the frequency nominal value, and the reserves that can be injected back into the grid when the frequency drops below the nominal value. The transfer function is modelled as a first-order with a small-scale time constant. Fast dynamics, such as pulse-width modulation (PWM), have been neglected in this model. If the time constant has a higher value, the frequency response could be affected, which influences the PFC response.

When the PHEV is in disconnected mode, there is no primary frequency control due to the disconnection from the grid, which implies that the participation factor is equal to zero. But from the behaviour patterns of PHEV uses, there will be a few vehicles connected during the day that will be involved in the primary frequency control.

The PHEVs state of charge asynchronously differs over time when in charging mode. Depending on the battery type, the charging could be constant voltage (CV) or constant current (CC) modes, as can be seen in Figure 3.4. These modes affect the participation of the PHEVs. During charging mode, the PHEV battery charger controls the DC link voltage.

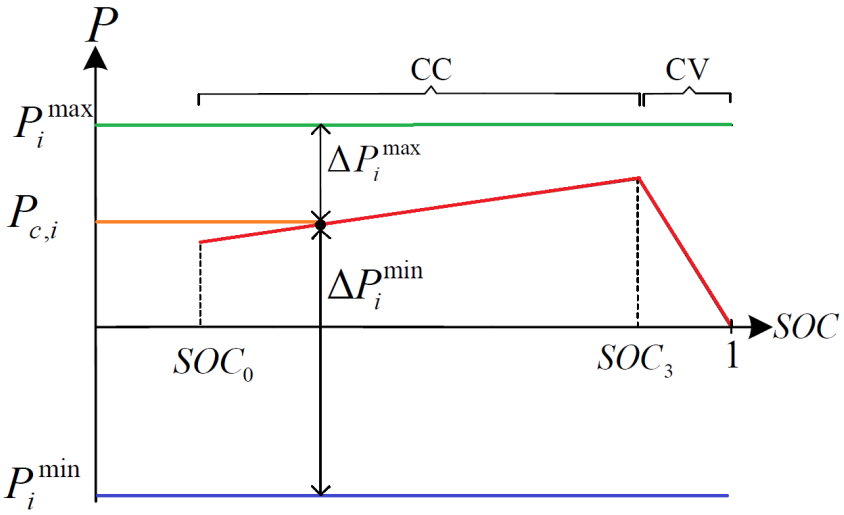

Figure 3.4: Li-ion battery vs state of charge – charging of power.

Due to the smart energy management of the aggregator, the PHEV can come to a halt when charging is completed or temporarily stopped for other reasons. The PHEV charging power could be equal to zero, even though they are connected to the power grid. During idle mode, the DC link voltage is equal to the terminal voltage of the battery. The idle mode can provide vehicle-to-grid services even though the charging power is equal to zero.

The graph in Figure 3.4 shows the PHEV being charged in constant charging mode from SOC_0 to SOC_3. The battery voltage slowly rises as the charging current remains constant. Steady increases of the SOC for the charging power of the PHEV occur. The charging modes change from constant current to constant voltage due to the PHEV reaching the voltage maximum threshold. The terminal voltage slightly increases and is near-constant for the PHEV until the batteries are fully charged and the SOC is equal to 1.

The graph in Figure 3.5 shows the charging mode of a typical Li-ion battery. Using the increase and decrease of the slope, the changes of the participation factor are avoided for SOC_a to SOC_b and SOC_c to SOC_d. Before the SOC_a, there is no primary frequency control due to the minimum state of charge of the battery. Charging power is fully controlled when in constant current charging mode between SOC_a to SOC_d. The charging mode changes from constant current to constant voltage when the state of charge is more than SOC_d in an open-loop configuration. When the battery is fully charged, at rated voltage, the control

secures the battery terminal voltage. Due to the open-loop, it is deduced that the participation factor is zero and the PHEV doesn't contribute to primary frequency control.

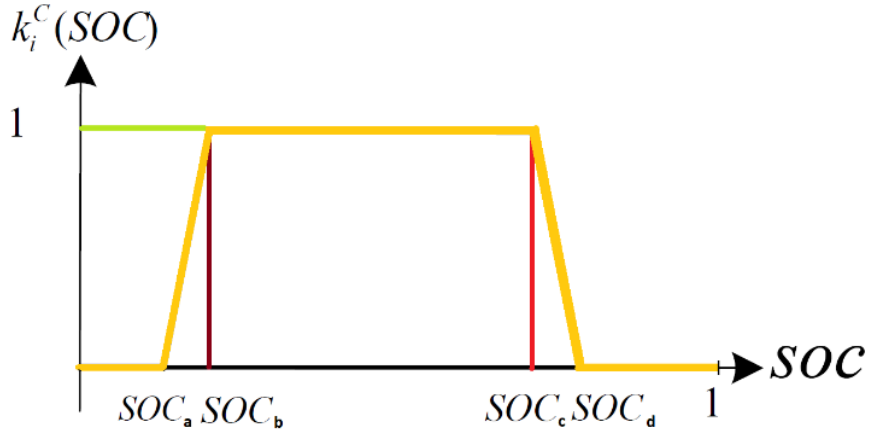

Figure 3.5: Charging mode showing participation factor vs state of charge.

3.1.4 Fractional Order PID Controller

The FOPID was widely used for methods in control theory and improved expiation of results. Similarly, the controller has the same benefits as conventional PID controllers, utilising proportional control to provide an immediate action to control error, integral control to use the constant error by driving it near to zero, and derivation control which acts upon the change of the error. The PID controller has the advantages of reducing steady-state error to zero, moderate peak overshoot, and moderate stability, and can be used for fast/slow process variables. The FOPID has similar characteristics, with the inclusion of integral and differential order λ and μ. This provides two additional adjustable parameters compared to the traditional PID controller as seen in the arrangement in Figure 3.6. The controller becomes more flexible in a control structure and can obtain a better control effect. The various control structures encompass gains for K_P, K_I and K_D as depicted in the figure below which were obtained using trial and error, and tuning app PID on MATLAB for the experimental study of the research. The arrangement of the controller modelled on MATHLAB is depicted below showing the five gains. Multiple iterations of the controller were done to discover optimal gain values.

$$K_c(s) = K_P + \frac{K_I}{S^\lambda} + K_D s^\mu, \quad \lambda, \mu > 0 \tag{3}$$

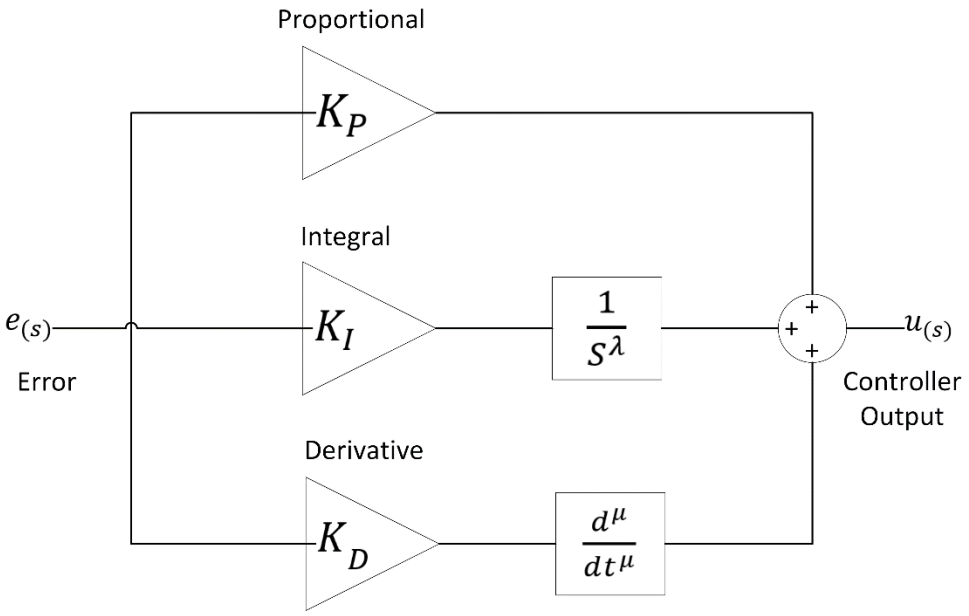

Figure 3.6: Arrangement and structure of FOPID controller.

3.1.5 Performance Index

The overall performance of the system can be accurately determined by the use of indices that can calculate the area of the error. It becomes difficult to compare the behaviour of signals through the illustration of the results and by doing an analysis of performance. These indices can assist researchers in optimisation and fine-tuning parameters to improve the results of isolated power system simulations. This will be dependent on whether a faster computational rate or less cost is required. In this research, the indices are used for comparison of the controller performance for ease of analysis. The formulas for the indices can be seen below:

Integral Square Error has less overshoot and undershoot in steady-state regions. They also have better robustness in steady states. This criterion can penalize large errors, particularly those that occur initially. The equation can be seen below:

$$ISE = \int_0^\infty e^2(t)\, dt \tag{4}$$

Integral Absolute Error has a higher convergence rate to achieve the best cost. This criterion treats all errors (large and small) the same. The equation can be seen below:

$$IAE = \int_0^\infty \left| e(t) \right| dt \quad (5)$$

Integral Time Square Error has better robustness in steady states. The equation can be seen below:

$$ITSE = \int_0^\infty te^2(t)dt \quad (6)$$

Integral of Time Absolute Error has less overshoot and undershoot in steady-state regions. This index also has a higher convergence rate to achieve the best cost and penalizes errors that persist for a long time. The equation can be seen below:

$$ITAE = \int_0^\infty t \left| e(t) \right| dt \quad (7)$$

3.2 Design of an Isolated Thermal Power System with RES and Application of Fuzzy Type-2 Fractional Order PID Controller

3.2.1 Introduction

The implementation of clean energy into the power system is the focus of the modern era. Multiple applications such as hydro, wind, and solar power are being interconnected with the existing power system to help curb some of the negative environmental effects. Renewable energy is known for its highly non-linear contribution to the grid. PV-based solar energy makes use of unlimited light energy from the sun, called irradiance. The energy output is dependent on the amount of irradiance that can be produced. This contributes to a highly variable system due to the fluctuations of sunlight that are available in a particular area. Further, wind energy has shown to have a similar effect with wind being highly unpredictable through constant wind speed variations. Even though this is the case, the global temperature was rising every year, making solar energy a good alternative for energy generation. Similarly, studies have shown that wind levels are bound to increase in the future.

When the RES systems are coupled with existing power plants, one of the frequency control methods used in this research is FOPID. This controller is shown to positively abolish steady-state error, transient disturbance reduction, system non-linearities, and uncertainties. With its multiple parameters that are required, but difficult to determine, manual tuning or algorithms are used to decipher the appropriate gains. The system's robustness and dynamic characteristics improve to a certain extent.

Optimisation techniques applied, such as particle swarm optimisation, have proven to positively affect results. Artificial intelligence used for this research optimisation has shown to utilise multiple methods structured from behavioural patterns of living organisms as a way to successfully solve uncertainties in the power system. Tuning of adaptive parameters by performing an input delay has also been illustrated to produce positive results for the load frequency of a two-area power system. By utilising a PID controller with FT2,

the output scaling factor has increased this research system performance and kept stability with input delay and uncertainties.

3.2.2 Isolated Power System Model

An interlinked isolated thermal power system with solar farms and wind farms connected to each area is shown in Figure 3.7, and an electrical single line diagram done on ETAP in Figure 3.8 to overview the arrangement in the power grid transmission. These areas are interconnected via an AC tie-line. Both areas have a isolated thermal power system which consist of a governor, turbine, and generator model that have the relevant parameter for gains and time constants.

The non-linearities present such as governor dead-band (GDB) and generation rate constant (GRC) have been included to consider the ramp rate constraints and upper-to-lower bound constraints. The signal from both areas connects to the synchronising coefficient via the tie-line and provides the relevant inputs and outputs for the rest of the isolated interconnected power system. The interconnected system integrates with primary control action, known as the speed governor mechanism, and the proposed FT2 FOPID. This controller uses multiple parameters for fine-tuning to reduce the uncertainties and disturbances in the system. The change in power demand is present in both area 1 and area 2 for analysis of the controller performance to bring the system back to steady-state condition i.e., frequency and tie-power deviations.

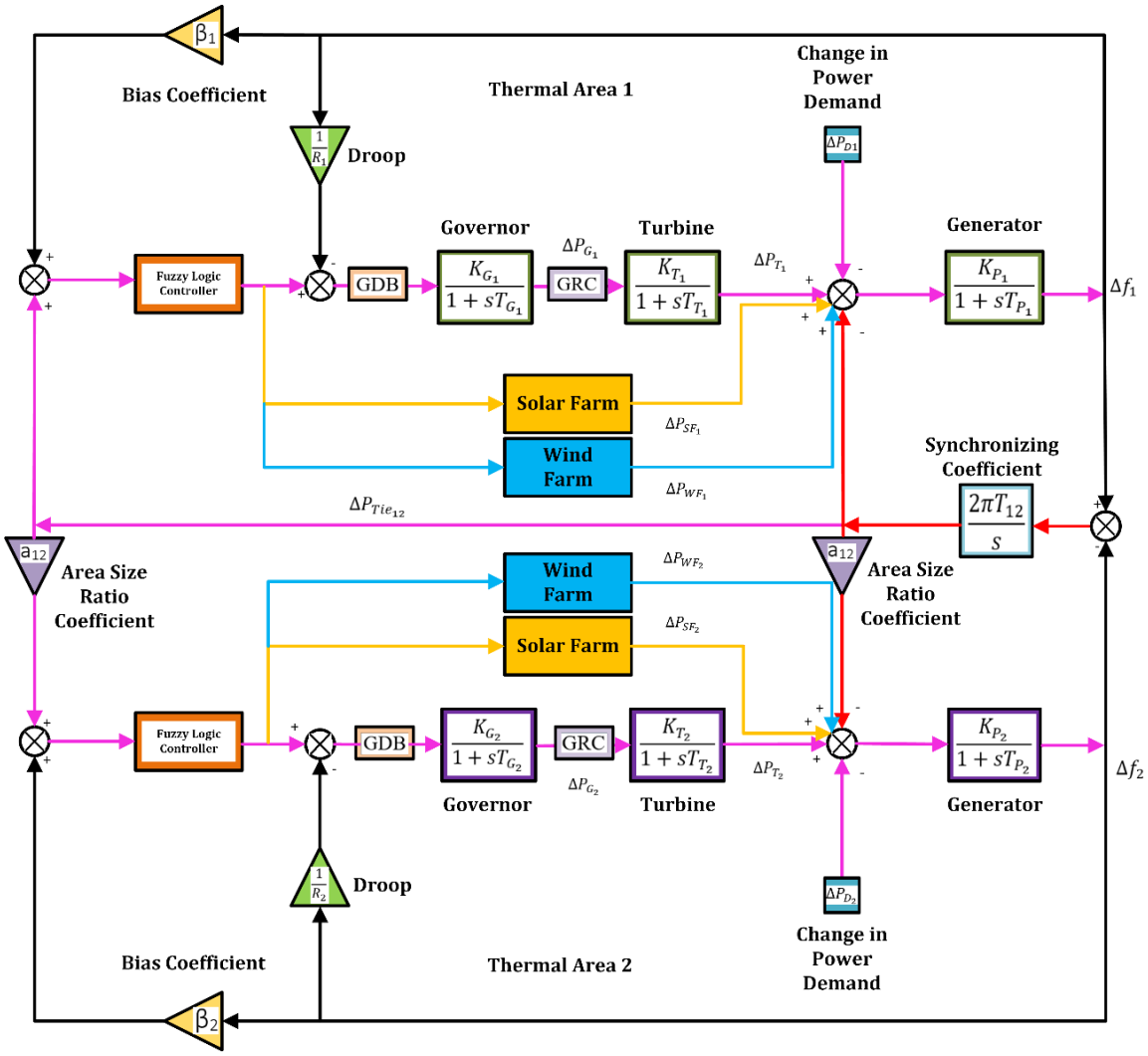

Figure 3.7: System model with RES.

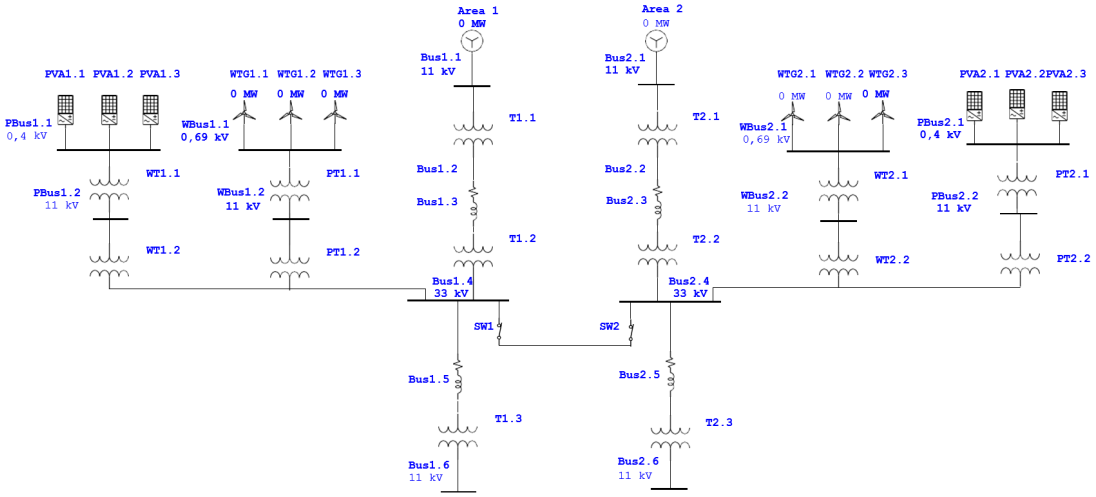

Figure 3.8: Single-line electrical diagram of interconnected system using ETAP software.

3.2.2.1 Governor Dead-band and Generation Rate Constant

A consideration called governor deadband (GDB) is integrated when there is minimum change in the turbine valve position due to undergoing speed fluctuations. The phenomenon of this non-linearity is as shown below: 0.05%

$$y = F\ (x, dx) \tag{8}$$

The hypothesis of x as a sinusoidal oscillation is justified due to the continuation of oscillations with a period of 2 seconds which can be seen in equation (9) where A is amplitude, ω_o is frequency oscillations where by $\omega_o = 2\pi(0.5) = \pi$.

$$x = A \sin \omega_o t \tag{9}$$

The Fourier series for the function $F\ (x, dx)$ is shown as:

$$F\ (x, dx) = F_o + Z_1 x + \frac{Z_2}{\omega_o} dx + ----- \tag{10}$$

It is considered sufficient to take into account the starting three terms since the non-linearity is symmetrical about the origin, DB represents the dead-band and F_o is zero. This can be seen in equation (11) below:

$$F\ (x, dx) = Z_1 x + \frac{Z_2}{\omega_o} dx = \left(Z_1 + \frac{Z_2}{\omega_o}\frac{d}{d_t}\right) x = DBx \tag{11}$$

The Fourier coefficients are Z_1 = 0.8 and Z_2 = -0.2. The dead-band is set at 0.05% in the isolated thermal power system model.

For protection of the electrical power system equipment from continues damage, the lower and upper generations can be changed only at a set out maximum rate. This is called generation rate constraint (GRC) which is coupled with the turbine of a isolated thermal power system. The GRC is adjusted at 3% for the isolated thermal power system. A basic block diagram can be seen in Figure 3.9 below:

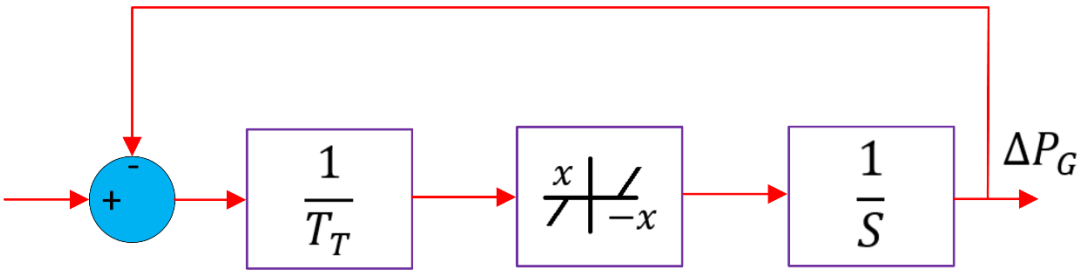

Figure 3.9: GRC non-linearity connected with turbine model.

3.2.3 Solar Farm Model

A PV system consists of the PV panel, maximum power point tracking (MPPT), sinusoidal pulse width modulation (SPWM) inverter, and filter. A solar cell panel is made up of semiconductors that have been doped to contribute to the deficit of free electrons on the reverse side, and surplus on the front side. This panel works with the photovoltaic process where photons are absorbed in the solar cells. The solar cell can produce an output voltage of 0.3-0.6V. This is dependent on the temperature and irradiance [31, 49-50]. An equation for the solar panel can be derived from equations (12) and (13) and shown below:

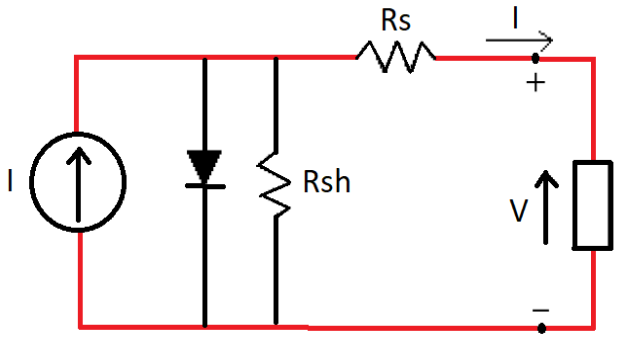

Figure 3.10: Solar cell equivalent circuit.

$$I = I_1 - I_0 \left(e^{\frac{(V-IR_S)}{AkT}} - 1 \right) - \frac{V-IR_S}{R_{SH}} \tag{12}$$

Where:

I = PV array output current

I_1 = Incident sunlight generated to array current

I_0 = Reverse saturation current of the PV array

V = Output voltage of the PV array

R_S = Equivalent series resistance of the array

R_{SH} = Equivalent parallel resistance of the array

A = Diode quality factor (ranging 0 - 2)

k = Boltzmann constant (1.380649×10^{-23} m^2 kg s^{-2} K^{-1})

T = Temperature (° C or K)

$$I_1 = \left(\frac{\lambda}{1000}\right)[I_{SC} + k_1(T - 25)] \quad (13)$$

Where:

λ = Irradiance (0 - 2500 $W.m^{-2}$)

I_{SC} = Short circuit current

The solar equivalent circuit is shown in Figure 3.10. To harness the maximum power from a solar panel, a method called maximum power point tracking (MPPT) is utilised to provide input voltage regulation and improve efficiency. The voltage can be regulated through a booster DC/DC converter to deliver maximum power to the load. This type of converter can provide a higher output voltage than input voltage, which is discovered with the duty cycle of the gate pulse to the MOSFET switch [36]. Boost converters have two modes - ON and OFF state modes - which are shown in equations (14) and (15) respectively.

$$ON\ STATE\ \left\{L\frac{di_1}{dt} = V_{PV}, C\frac{dV_0}{dt} + \frac{V_0}{R} = 0 \right. \quad (14)$$

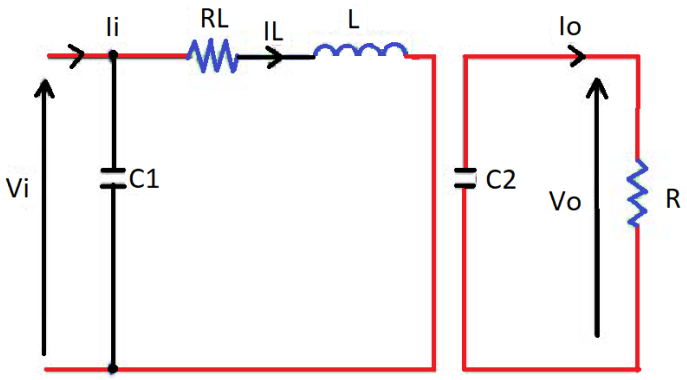

Figure 3.11: ON state operation.

$$OFF\ STATE\ \left\{L\frac{di_2}{dt} + V_0 = V_{PV}\,, i_2 + C\frac{dV_0}{dt} + \frac{V_0}{R} = 0 \right. \quad (15)$$

Where:

i_2 = Current in the inductor (A)

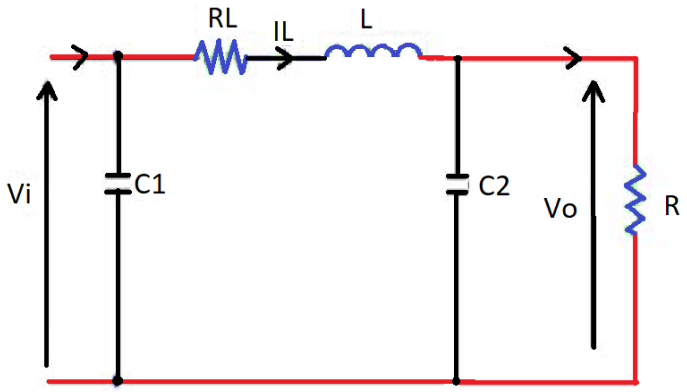

Figure 3.12: OFF state operation.

The ON and OFF state operations are shown in Figure 3.11 and 3.12. For the conversion of DC to AC power, an inverter is utilised in this application. The sinusoidal pulse width modulation inverter is used to maintain the constant voltage. Finally, a filter is used to remove disturbances within the output power signal. From these components, a transfer function equation is derived, seen in equation (16), with the structure of the equation can be seen in Figure 3.13.

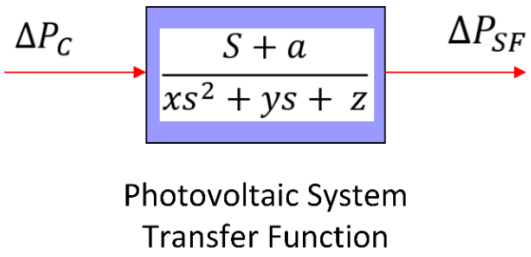

Figure 3.13: Model of photovoltaic panel transfer function.

Depending on the type of PV cell being used, the PV panels in general have a very low efficiency, which is approximately 18 to 30%. To maximise the power output and make the most of the solar energy given from the sun, maximum power point tracking is required.

From the information shown in Figure 3.14, the irradiance levels indicate that South Africa can use solar energy. While the panel generation factor (PGF) for desert locations is 3.86, and tropical coastal climate is 3.43, the cloud cover can affect the irradiance levels of areas. This has an impact on the power produced by solar panels. The tilt angle of the panels has to be considered for maximum power output due to the changing seasons throughout the year. The recommended angles for solar panels are 49^{o} tilt for winter, and 19^{o} for summer, to have the most irradiance that can be harnessed by the panels. Considering all these factors, for the modelling of solar PV, an average of 1000W/m^2 for solar radiation is considered. The transfer function for a solar PV system considering the PV panel, MPPT, sinusoidal pulse width inverter and filter can be seen in equation (16) obtained from [32].

$$P_{PV} = \frac{-18s+900}{s^2+100s+50} \tag{16}$$

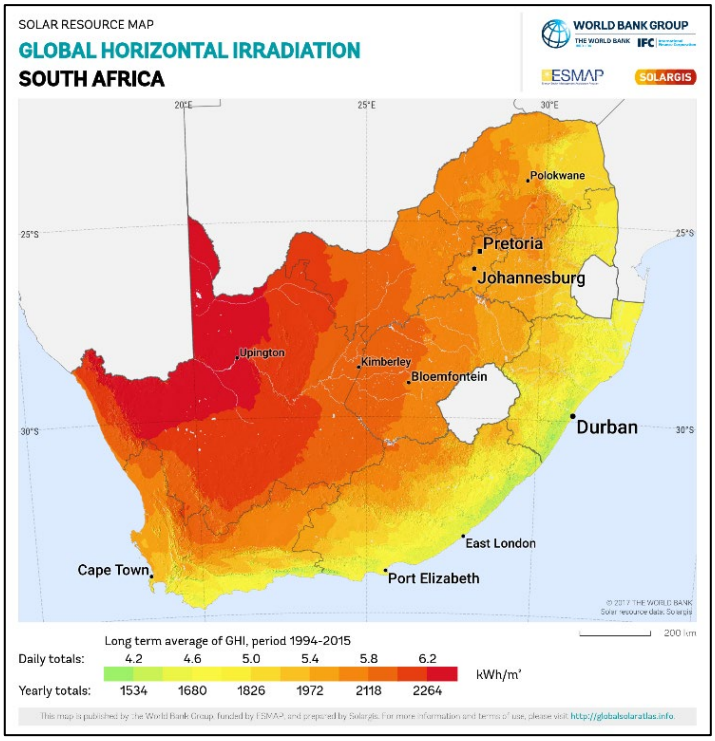

Figure 3.14: Irradiance level of South African multiple regions taken from Solar GIS 2022 online software [93].

3.2.4 Wind Farm Model

DFIG can contribute to frequency regulation, but the frequency changes of the wind turbine were ignored earlier due to the separate inertia. The operations are controlled via electronic controllers for communication between the grids. Power reserve control using speed and pitch can assist with frequency control in the power system.

The DFIG releases kinetic energy to support system inertia due to the additional inertia control loop that creates frequency sensitivity in the system. Governor setting and system inertial response is researched for the frequency control of DFIG. Extracting the kinetic energy of the turbine blades from DFIG-based wind turbines contributes to the reduction of the rotor speed, which responds to the deviation of frequency to improve the frequency of the power system [21-23]. When only tracking using non-conventional machine-equivalent controllers, the inertial control adds a signal to the power reference output in equation (17) according to [23]. The frequency behind a high-pass filter is represented as Δf, constant weighting the frequency deviation derivative is K_{df}, and the frequency deviation as K_{pf}. When the frequency transient is over, the equivalent non-conventional machine moves back to the optimal speeds. By forcing the speed to track the desired speed reference, a power reference is used in equation (18). The PI controller is utilised with design constants of K_P and K_I. This controller is for fast recovery speeds and transient speed variations. For non-conventional generators, from equations (17) and (18), the total active power reference for non-conventional generators is in equation (19). In a short period of time, frequency transients generally occur. A slow PI controller is provided by p_{ω}^{*}. There are no dynamics in the power reference p_f^* and non-conventional total power injection if the power p_{NC} is regulated by high-speed power electronics. The equation can be seen in (20). The injected power before the frequency transient is shown as p_{NC}^{0}. The inertial control affects the power system. The system damping is provided by K_{pf} and system inertia is regulated by K_{df}. The non-conventional generating machine contributes to system inertia and, in conventional inertial control, the system inertia converts to H^* as shown in the equation (21). The modified inertial control for a DFIG is given in equation (22). Using a washout filter for the change in frequency having time constant T_{ω}. The reference point is shown in equation (23). The frequency change measured where the wind turbine connects to the network is ΔX_2, and R is the speed regulation. Using the stored kinetic energy, the change in frequency during

load disturbance is detected by the DFIG. The proposed controller provides fast, active power injection control. During any disturbance, active power is injected by the wind turbine is ΔP_{NC}. By maintaining the reference rotor speed where maximum output power is obtained, the power injected by wind turbine is differentiated with $\Delta P_{NC,ref}$. The wind turbine mechanical power is shown in equation (24). The model of the DFIG system shown in Figure 3.15. The wind model is made up of frequency measurement, washout filter, droop, speed controller, mechanical inertia, and finally, the wind turbine.

$$P_f^* = -K_{df}\frac{d\Delta f}{dt} - K_{pf}\Delta f \tag{17}$$

$$P_\omega^* = K_P(\omega_e^* - \omega_e) + K_I\int(\omega_e^* - \omega_e)\,dt \tag{18}$$

$$P_{f\omega}^* = \left[-K_{df}\frac{d\Delta f}{dt} - K_{pf}\Delta f\right] - [K_P(\omega_e^* - \omega_e) + K_I\int(\omega_e^* - \omega_e)\,dt] \tag{19}$$

$$P_{NC} = \left[-K_{df}\frac{d\Delta f}{dt} - K_{pf}\Delta f\right] - P_{NC}^0 \tag{20}$$

$$(2H + K_{df})\frac{d\Delta f}{dt} = P_f - D\Delta f = P_G + P_{NC} + P_T - P_L - (K_{pf} + D)\Delta f \tag{21}$$

$$\frac{2H}{f}\frac{d\Delta f}{dt} = P_f - D\Delta f = P_G + P_{NC} + P_T - P_L - D\Delta f \tag{22}$$

$$P_f^* = \frac{1}{R}(\Delta X_2) \tag{23}$$

$$P_{mech} = \left(\frac{\frac{1}{2}(\rho Ar)}{S_n}C_{p.opt}\right)\omega_s^3 \tag{24}$$

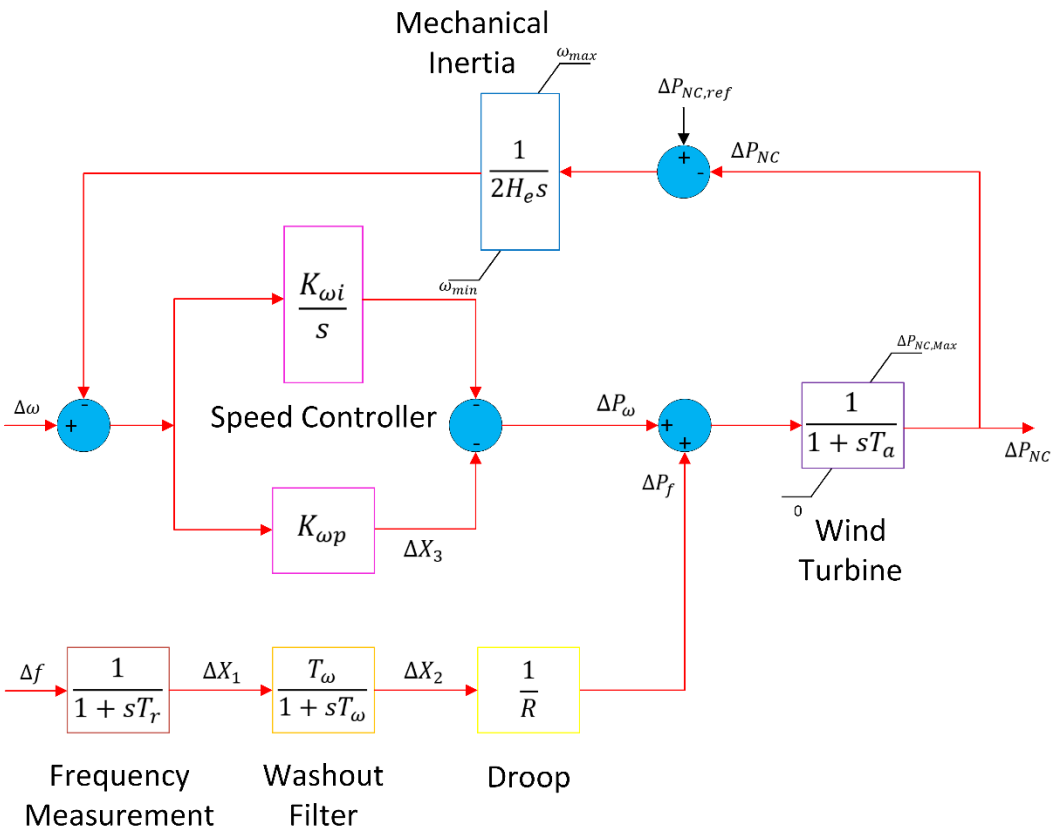

Figure 3.15: DFIG wind turbine model with inertia control.

The winds levels as shown in Figure 3.16 provides as indication in which month the wind power system becomes more desirable which is September, October and November. The wind speeds fluctuate and rarely go above 38 km/h which shows its inconsistency, efficiency and non-linearity that it provides to the power generation therefore proving that coordinated control is required.

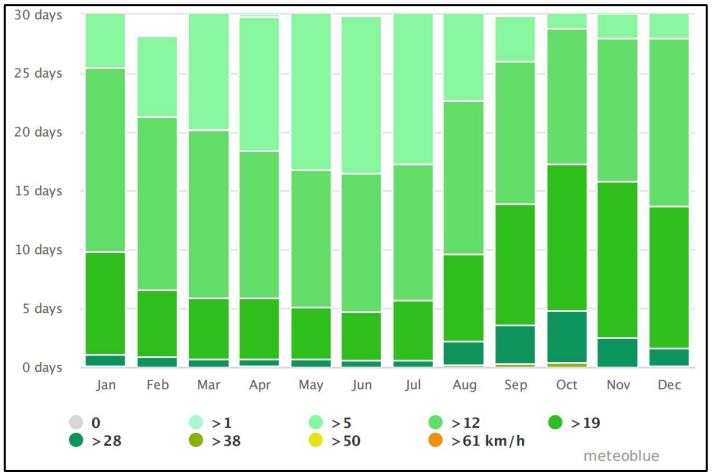

Figure 3.16: Wind speed levels during the course of the year for South Africa 2021 taken from Meteoblue weather online monitoring [94]

3.2.5 Fuzzy Type 2 Fractional Order PID Controller

The controller consists of a FOPID together with fuzzy action due to its positive advantages in solving disturbances and stability applications. The tuning of FOPID consists of five parameters which are K_P, K_I, K_D, λ, and μ. These parameters are highly variable to the output, and complex so they require tuning via the well-known particle swarm optimisation (PSO).

The chosen variables are selected to provide the best possible outcome for the controller. Further various optimisation techniques can be utilised, but are not guaranteed to provide optimal outputs. Through fractional calculus, more adjustable parameters can be provided, which assist with tuning the controllers. The flexibility, stability, and control effect are improved with FOPID, which acts as a filter for an infinite dimension. FOPID has a memory function that is related to all history in the fractional differentiation. The far and close errors have smaller and larger response factors respectively. The future and present information are influenced through this. Therefore, this provides good applications for boiler-turbine systems. The arrangement done on MATHLAB of the controller can be seen below in Figure 3.17.

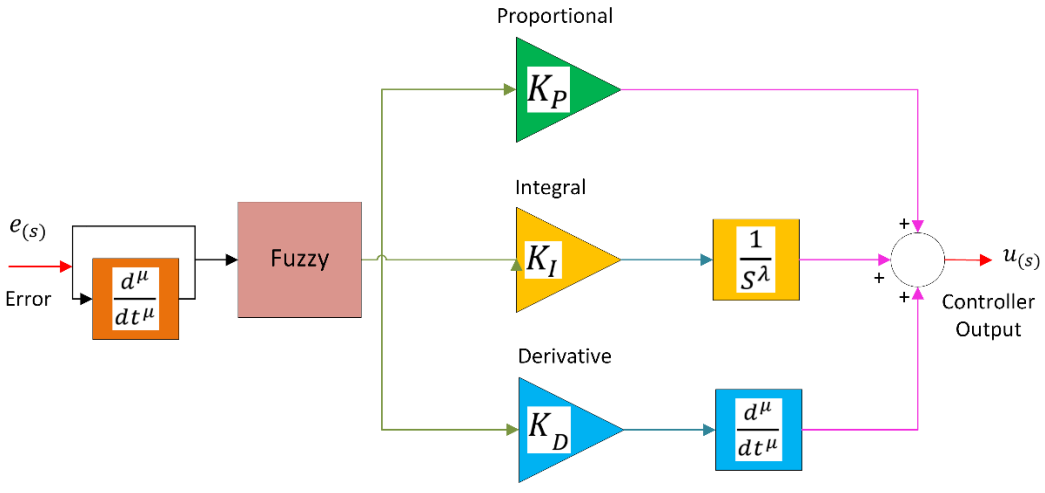

Figure 3.17: Fractional order fuzzy logic controller.

The FT2 controller consists of five elements that make up this controller. Those elements are fuzzifier, fuzzy interference, fuzzy rules, type-reducer and defuzzifier as seen on Figure

3.18. Each process contributes an important role in the output of data. The input of data is fuzzified through the introduction of membership functions for ease of understanding and classification. The data is changed to a fuzzifying input through the use of fuzzy applications into membership functions to establish a rule strength. The Mamdani fuzzy interference system is used due to its advantages such as intuitiveness, widespread acceptance, and interpretable rule base. Combining the rule strength and the output membership function to find the consequence of the rule is Mamdani FIS. The structure of a fuzzy type-2 is similar to FT1 as seen on the figure below, with the only difference being the type reduction process function, which provides better controller handling system uncertainty because it can model them and minimise their effect. If all uncertainties disappear, the FT2 sets convert to type-1 which thereafter gets the final defuzzification result.

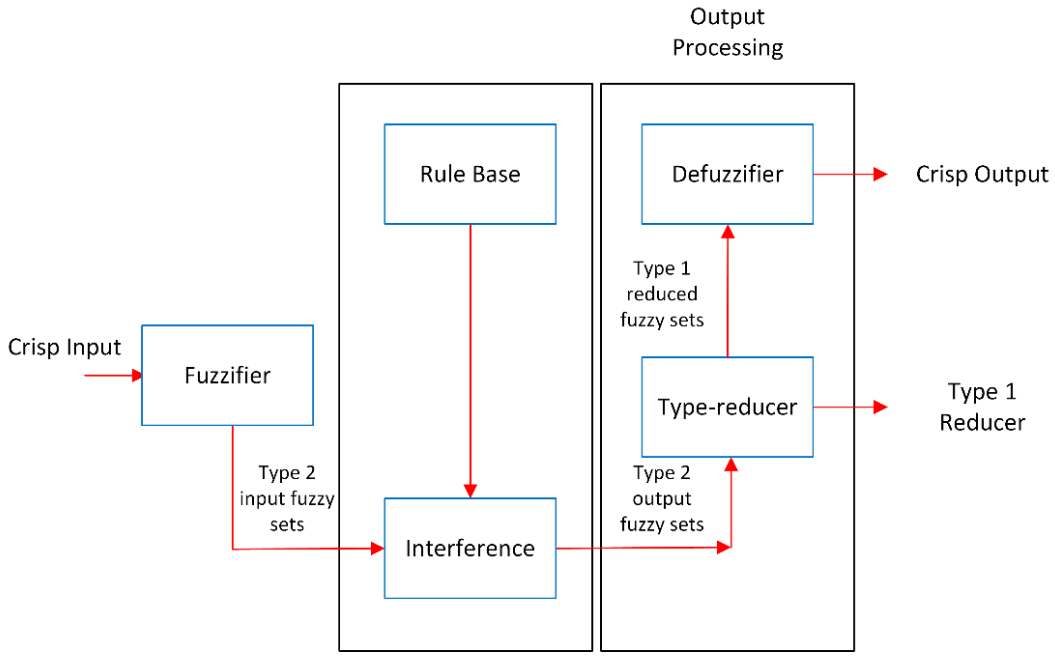

Figure 3.18: Fuzzy type-2 logic system block diagram [80]

For this research, the Nie-Tan method (NT) type reduction was utilised with no iterative process which improves type reduction efficiency. A FT2 has more design degrees of freedom than a FT1 because type-2 has more parameters than type-1. As random uncertainties flow through a system, their effects can be evaluated using the mean and the variance. Linguistic and random uncertainties flow through a FT2, and their effects can be evaluated using the defuzzified output and the type-reduced output of that system. Often

used in intervals, the variance provides a measure of dispersion about the mean. The defuzzified output, which provides a measure of dispersion, is the interpretation of the type-reduced output. The type-reduced set also increases as linguistic or random uncertainties increase, and the variance increases as the random uncertainty increases. A FT1 is comparable to a probabilistic system through the first moment, whereas a FT2 is comparable through the first and second moments. The rules are based on the individual's application of the information data. The fuzzy yield is made up of 49 laws from seven triangular membership functions on information and yield data. The logic statements "if" and "then" are used to determine the yield at that point. These rule base have been utilised for FT2-FOPID which can be seen in Tables 3.3. The output distribution is defuzzified to produce crisp outputs. The membership functions are generally used from negative one to positive one, and the design membership functions for error and error deviation are shown in Figure 3.19.

Table 3.3: Fuzzy type-2 FOPID rule base.

ACE/ dACE	**NB**	**NM**	**NS**	**ZE**	**PS**	**PM**	**PB**
NB	NB	NB	NB	NB	NM	NS	ZE
NM	NB	NB	NB	NM	NS	ZE	PS
NS	NB	NB	NM	NS	ZE	PS	PM
ZE	NL	NM	NS	ZE	PS	PM	PB
PS	NM	NS	ZE	PS	PM	PB	PB
PM	NS	ZE	PS	PM	PB	PB	PB
PB	ZE	PS	PM	PB	PB	PB	PB

The rules are based on the Boolean system of true or false statements to provide valuable flexibility for reasoning, thereby considering the inaccuracies and uncertainties in the system. In a fuzzy logic system, there is no absolute true or false, but it is partially true or false. The rule base contains "if" and "then" conditions to govern the decision-making system, which is very important for the output results. The rules are inputted into the interference that matches the current fuzzy inputs, with each rule statement that produces the required outputs to perform control actions. This helps remove uncertainties and disturbance to a level that is acceptable. Some of the rule base statements are shown in

Table 3.4 where the two inputs are checked against the interference system, which consists of the set of rules and the output of the type reducer.

Table 3.4: Rule base statements.

Rule	Statement
1	If ACE is A and dACE is A then dACE is NB
2	If ACE is B and dACE is A then dACE is NM
3	If ACE is C and dACE is A then dACE is NS
4	If ACE is D and dACE is A then dACE is ZE
5	If ACE is E and dACE is A then dACE is PS
6	If ACE is F and dACE is A then dACE is PM
7	If ACE is G and dACE is A then dACE is PB

The input values of a FT2 have membership functions ranging from upper membership function to lower membership function. This provides two fuzzy values for each type-2 membership function. With the rules discussed previously, the fuzzy operator is applied to the fuzzified values of the membership functions. The minimum and maximum output value for the fuzzy set of each rule is the result of the fuzzy operator to the fuzzy values of upper and lower membership functions.

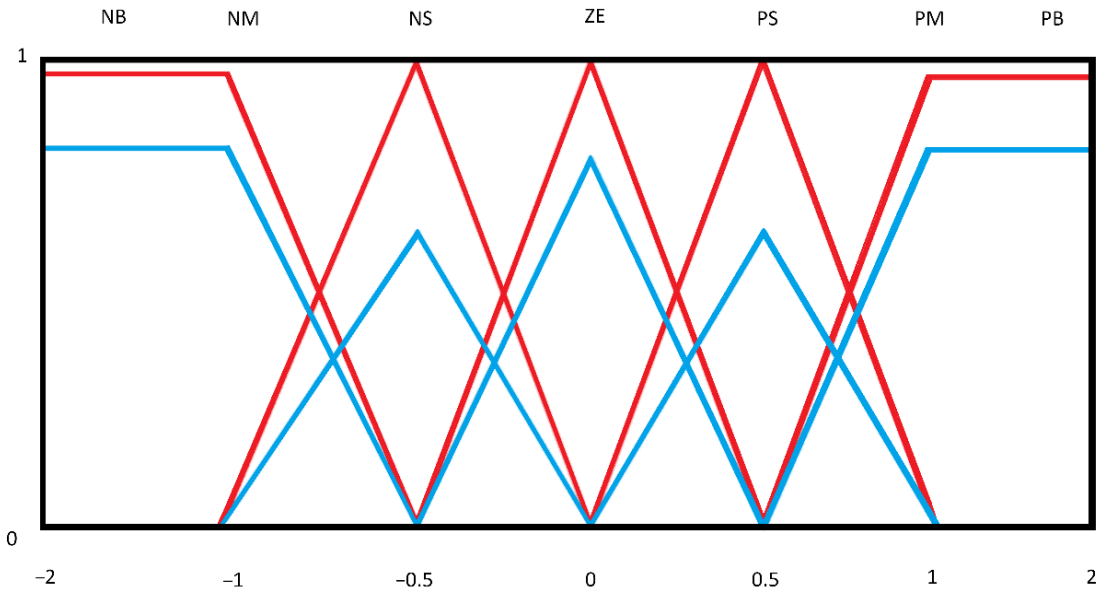

Figure 3.19: Fuzzy type-2 primary membership function of error and error deviation.

3.3 Design of an Isolated Thermal Power System with PHEVs and RES Using the Application of Neural Network Predictive Controller

3.3.1 Introduction

The expansion of clean energy is becoming more relevant to society as we strive to become a fossil fuel-free country and reduce carbon emissions to zero. Excessive costs have derived from the release of greenhouse gases, and the availability of crude oil used for multiple types of transportation. Alternative resources are been researched daily to transfer into a new way of energy generation and mobility.

RESs, such as wind and solar energy systems, are considered unpredictable, with fluctuations occurring due to the changes in seasonal characteristics. Coordination is thereby required to manage and control these fluctuations to obtain the highest efficiency for power generation. Recently PHEV aggregator has become a part of the power system with the introduction of smart technologies providing two-way power flow. The PHEVs are becoming more commonly used in society where fossil fuel costs are exceedingly high and CO_2 reduction is of high importance.

By utilising advanced control methods in this research such as FOPID, Fuzzy integrated control and NNPC, the system is able to return to its original state at a faster rate. While the PHEVs does support the power grid to some extent, when multiple systems are connected together, additional control is still required. The analysis of each controller has on the system is therefore analysed in this research to understand the behaviour, outcome and effectiveness to curb disturbances in the system.

3.3.2 Isolated Power System Model

The tie-line for two isolated power systems is interconnected to allow two-way power flow between the two areas. The model shown in Figure 3.20 displays the transfer functions with the inclusion of the PHEVs.

A reheat turbine is part of the isolated thermal power system with its interconnected clean energy systems, due to its capability of increasing efficiency by returning the steam to the steam generator for reheating to the set temperature. Thereafter, the steam will be sent back to the turbine. This high-temperature steam is released as excess from the turbine due to high pressure

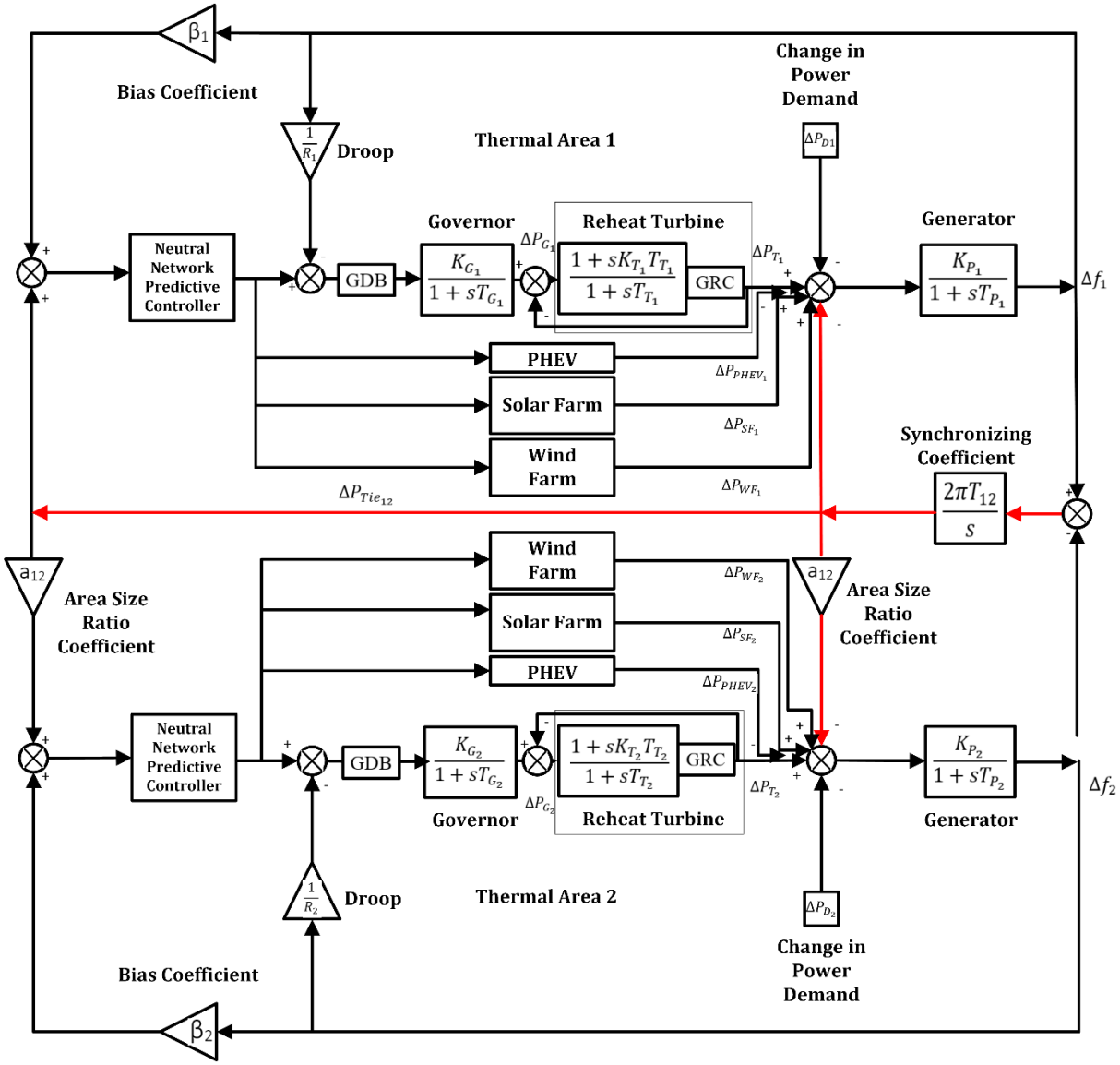

Figure 3.20: Clean energy systems interconnected with an isolated thermal power system.

3.3.3 Neural Network Predictive Controller

The controller used to remove the isolated interconnected power system non-linearity is called a NNPC, which predicts future power system performance. The controller over a stated future time horizon calculates the control input that will optimise the isolated power system execution. The controller, firstly, trains a neural network to represent the forward dynamic of the isolated power system. The predictive error between the neural network output and isolated power system output is used as the neural network training signal. This can be seen in Figure 3.21.

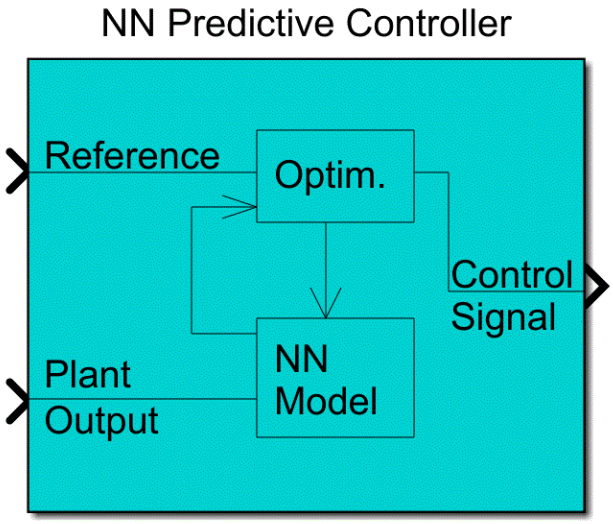

Figure 3.21: Simulink block of neural network control.

The future values of the isolated power system output utilise earlier inputs and outputs from the neural network isolated power system model. The network can be offline trained using the previously collected data from the operation of the isolated power system. The batch training algorithm used in the isolated power system is called multilayer shallow neural networks and backpropagation training. The workflow can be seen in Figure 3.22.

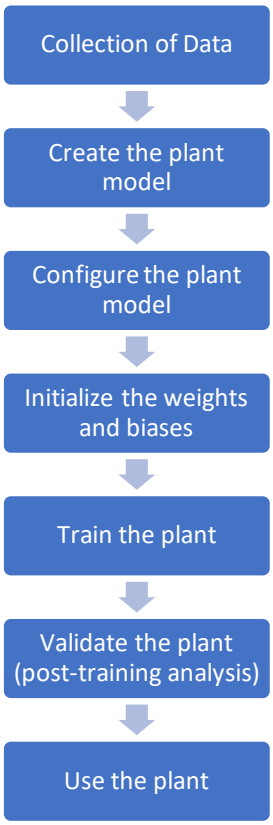

Figure 3.22: Workflow of general neural network architecture.

For a multilayer shallow neural network architecture, a logsig neuron with Z number of inputs, is weighted with an appropriate Y. The total of the weighted inputs and the bias forms the input to the transfer function, as seen in Figure 3.23. An output layer of linear neurons has more than one hidden layer of sigmoid neurons for feedback networks. Log sigmond transfer function generates outputs from 0 to 1 as the neuron's total input goes from negative to positive infinity. The network is allowed to learn non-linear connections between input and output vectors from multiple layers of neurons with non-linear transfer functions.

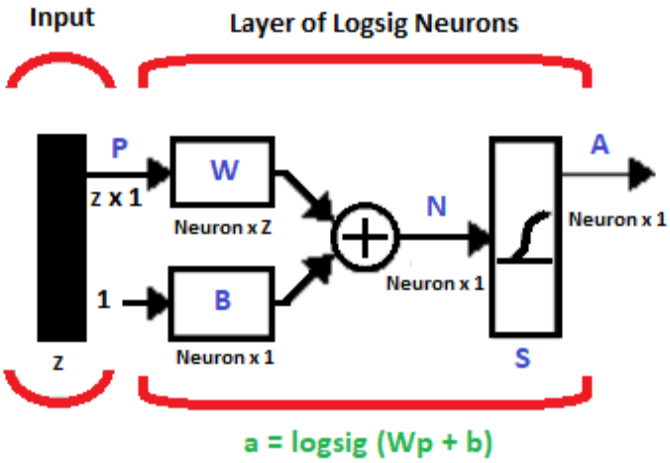

Figure 3.23: Feedback neural network structure.

3.4 Chapter Summary

This chapter discusses the isolated power system setup for each scenario with the RES and PHEV sub-systems modelled. The controllers used for each configuration explain the arrangement and the method of how they work to improve output. These designs are modelled in MATLAB/Simulink, and a comparison of performance is simulated and analysed in the next chapter.

4. RESULTS AND DISCUSSION

4.1 Isolated Two Area Thermal Power System with PHEV

The study work focal point is to determine the analysis of the different controllers being used and the effect of PHEVs on the isolated thermal power systems which are interconnected via a tie-line to satisfy the demand of the control areas. The model is used for evaluation of the demand change of 1% in area 1 within the two-area interconnected system. This is compared with the various PD, PI, PID, FOPID and finally FOPID controllers with PHEVs. The simulated results showcasing the frequency variations in area 1, area 2 and tie-line are displayed in Figures 4.1 to 4.3. For further comparison and results, a change in demand for both area 1 and area 2, with 1% and 2% respectively, were modelled for the study, which is graphically displayed in Figures 4.4 to 4.6. This was done to understand the behaviour of the controllers and the performance influence of the PHEVs in both areas.

Table 4.1: ITAE results obtained for various controllers for demand change of 1% in area 1.

Controllers	**Two-area System**		
	Area 1	**Area 2**	**Tie-line**
PD	16.68	16.25	6.17
PI	0.6433	1.656	0.7546
PID	1.104	0.5053	0.07105
FOPID	0.2165	0.1392	0.06173
FOPID with PHEV	0.1042	0.07045	0.02994

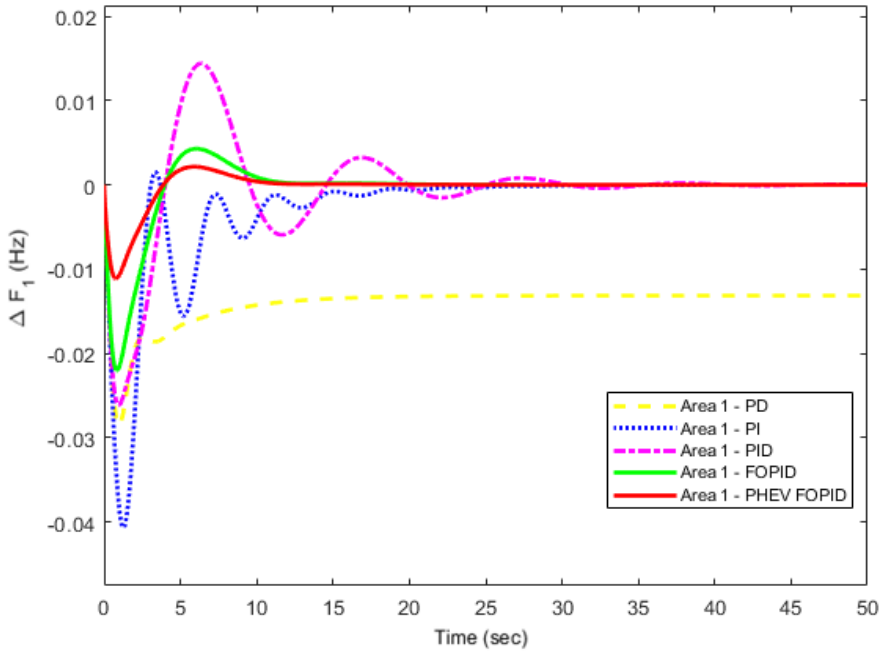

Figure 4.1: Area 1 - System frequency results for 1% load disturbance in area 1 using various controllers.

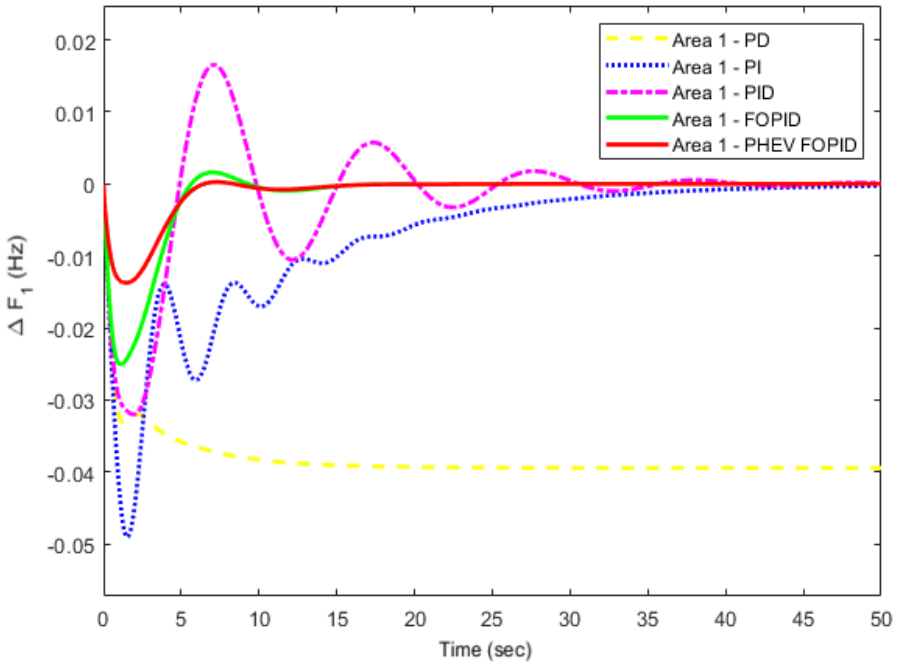

Figure 4.2: Area 1 - System frequency results for 1% load disturbance in area 1, and 2% load disturbance in area 2 using various controllers.

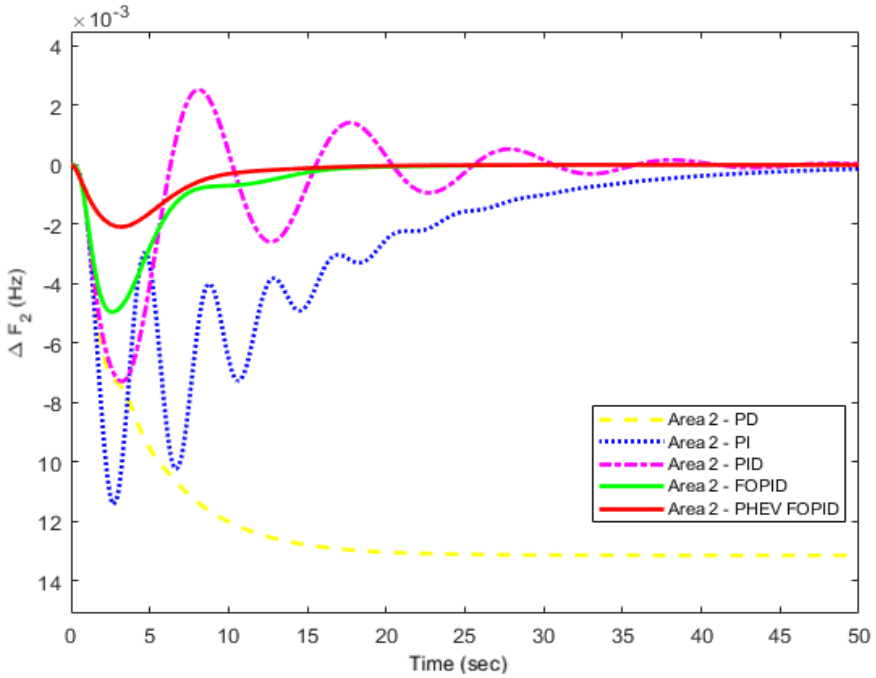

Figure 4.3: Area 2 - System frequency results for 1% load disturbance in area 1 using various controllers.

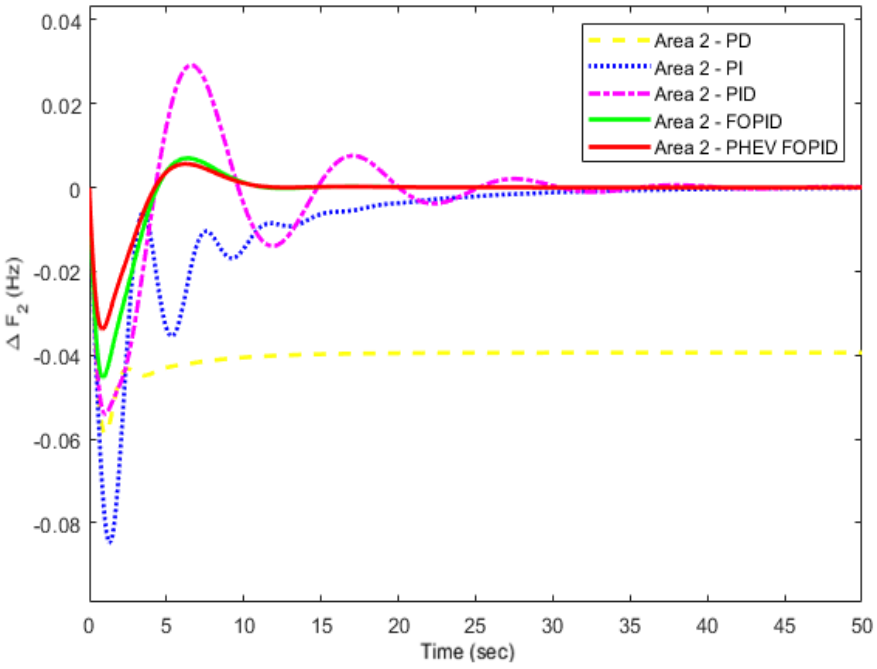

Figure 4.4: Area 2 - System frequency results for 1% load disturbance in area 1, and 2% load disturbance in area 2 using various controllers.

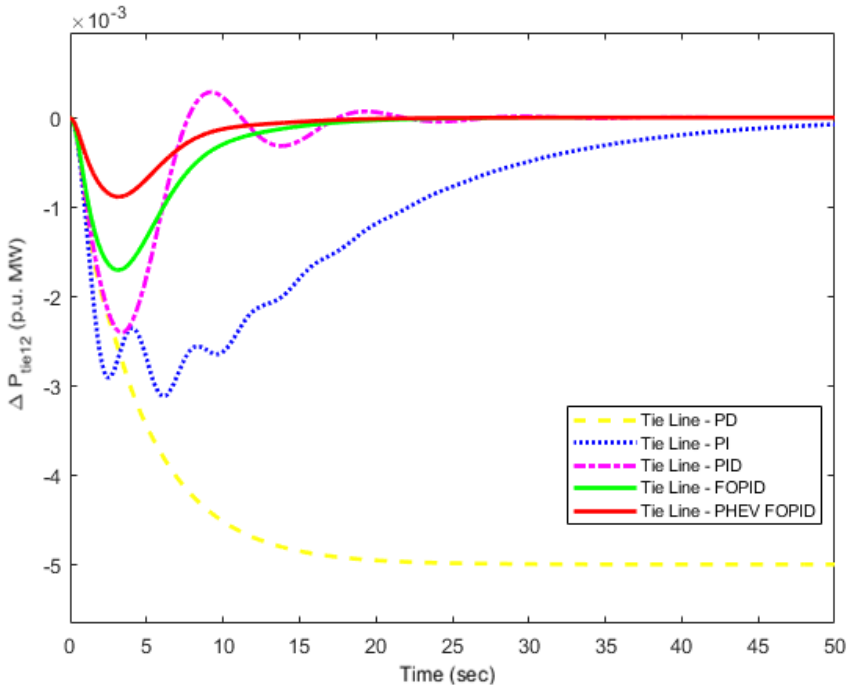

Figure 4.5: Tie-line - System frequency results for 1% load disturbance in area 1 using various controllers.

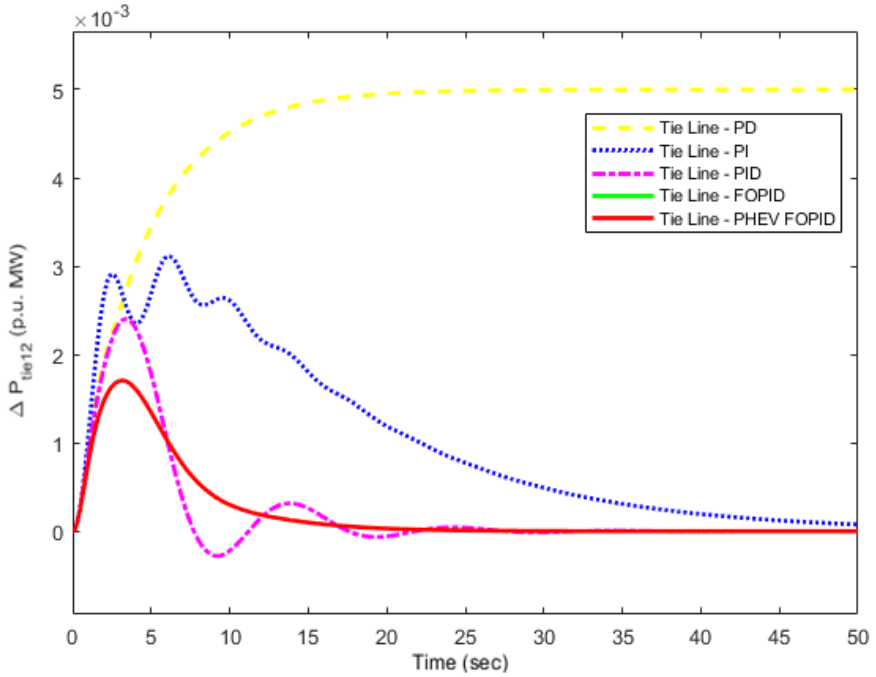

Figure 4.6: Tie-line - System frequency results for 1% load disturbance in area 1, and 2% load disturbance in area 2 using various controllers.

For simulation 1 where the load demand changes in Area 1 only and simulation 2 where the load demand is changed in both areas , the responses of PI, PD, PID, FOPID and FOPID PHEV is similar but has minimum changes for certain controllers.

From the data on Table 4.1, the results display that there is a scaled-down value of ITAE for FOPID with PHEV compared to the other controllers for differentiation and performance of the LFC. The FOPID tie-line (0.06173) is shown to have a low value compared to PI (0.7546) and PD (6.17).

The PD controller has a huge ITAE, and the results are clearly shown that the error still exists in the system response, which is not suitable for consideration. PI has displayed multiple oscillation for a duration of 20 seconds, which is not recommended. The ITAE for PID in area 1 (1.104) is very high compared to the few other controllers, due to the overshoot.

When comparing demand changes for the two simulations, PD is not returning to steady state and exceeds the run time of 50 seconds. The overshoot in Figures 4.6 and undershoot in Figures 4.1 to 4.5 is the highest compared to the other controllers but oscillations are not present. The PI controller has overshoot in Figures 4.6 and undershoot in Figures 4.1 to 4.5 which is the second highest and has 15 seconds of oscillations that are present. The wavelength is also greater for the dual load demand change simulation. The system comes back to steady state in Area 1 for the single load demand change at 30 seconds and Area 2 for the load demand change in the two areas at 45 seconds. The tie-line graphical outputs show that PI doesn't come back to it original state.

The PID controller brings the system back to steady state in all the simulation outputs. The graphical outputs for Area 1 and Area 2 shows that the system returns at 40 seconds whereas the Tie line graphical outputs returns at 30 seconds. The results for Figures 4.1 to 4.6 show that PID controller has oscillations, overshoot and undershoot that are present. The FOPID controller has minimum overshoot and undershoot in all graphical outputs. The output has also shown that the FOPID with PHEVs is free from oscillations for frequency and tie-line power, which is favourable for the power quality of the system.

Area 1 for the two load change simulations has a settling time of 15 seconds. The Area 2 for the load change simulations differ with the single load demand change output has a settling time of 17 seconds and dual load demand change outputs has a settling time of 13 seconds. The frequency doesn't exceed (±0.02) Hz in both areas.

With the inclusion of PHEVs, the results is similar to FOPID but with a drastic decrease to the overall error. With minimum overshoot and speedy settling time at 7 and 11 seconds, the PHEVs still show an enhancement of stability for both areas with load disturbances on single or both isolated power systems. The PHEVs have been shown to assist the frequency positively for both areas and tie-line, by reducing the overshoot and steady-state error at a moderate value. The controllers have been shown to have different overshoot peaks. The controller selected has shown to be superior to other controllers in its performance while introducing load alteration in both areas.

4.2 Isolated Two Area Thermal Power System with RESs

The research work displayed shows the analysis of the isolated thermal power system integrated with PV and wind-based power generation in each area, which is connected via an AC tie-line that contributes to the role of balancing supply and demand loads. The frequency of the designed interconnected system is analysed and studied for the behaviour of the signal. The investigation is meant to demonstrate the integration of clean energy through renewable energy sources effectively, within existing isolated thermal power systems, while assisting with variable load changes within the grid. Analysis with thermal power system no RES was used as a control to demonstrate the effects of RES penetration into the system and validate researched literature. Each control area action is limited by using the GDB and GRC non-linearities as it makes the action of secondary controllers more practical and realisable.

For this work, the controller FT2-FOPID is showcased. While the FT2 can be coupled with either PI, PD or PID, the FOPID was proven to provide favourable results in control problems due to the two additional freedom adjustable parameters. FOPID and FT1-FOPID are shown to have difficulty in dealing with the uncertainty of systems, therefore FOPID with type-2 fuzzy was applied. The controllers aim to restore the frequency and power deviations over tie-lines to their original state, within the least amount of time, while producing less settling time, low overshoot, and no oscillations. The different types of controller configurations are used for the comparison of the outputs. The ACE and dACE are inputs of the fuzzy system.

The output of the fuzzy is made of seven areas; NB, NM, NS, ZE, PS, PM, and PB. These are used within the triangular uncertainty member function class for ease of understanding. The reduced rule base with non-linear membership functions for FT2 is shown in Table 3.4 and Figure 3.19 in Chapter 3. The output of the fuzzy logic is defuzzified as type-1 reduced sets, which produce real values from crisp values. The input of the FOPID is coming from the output signal of the fuzzy logic system. The parameter gains for the FOPID that is K_P, K_I, K_D, λ, and μ are calculated through PSO with 50 iterations to produce the best results.

The simulated results are quantitatively given using the performance index Integral of Time Absolute Error (ITAE) and Integral Absolute Error (IAE). These indices can calculate the

area of the error which assist with higher accuracy for the analysis of the controller performance, especially in graphical representations. The comparison of performances was done using the output values given in Tables 4.2 to 4.5.

Table 4.2: ITAE results obtained for various controllers for demand change of 1% in area 1.

Controllers	**ITAE**
PID with no RES	0.9433
PID with RES	2.269
FOPID with RES	0.02066
FT1-FOPID with RES	0.01362
FT2-FOPID with RES	0.009286

Table 4.3: ITAE results obtained for various controllers for demand change of 1% in area 1, and 2% in area 2.

Controllers	**ITAE**
PID with no RES	2.093
PID with RES	4.057
FOPID with RES	0.06176
FT1-FOPID with RES	0.0401
FT2-FOPID with RES	0.02749

Table 4.4: IAE results obtained for various controllers for demand change of 1% in area 1.

Controllers	**IAE**
PID with no RES	0.05726
PID with RES	0.08157
FOPID with RES	0.007249
FT1-FOPID with RES	0.001953
FT2-FOPID with RES	0.001161

Table 4.5: IAE results obtained for various controllers for demand change of 1% in area 1, and 2% in area 2.

Controllers	**IAE**
PID with no RES	0.1139
PID with RES	0.1638
FOPID with RES	0.02205
FT1-FOPID with RES	0.005757
FT2-FOPID with RES	0.00347

The integrated and isolated power system is simulated using a 1% load demand change in area 1 for analysis purposes. The results of all the areas can be seen and arranged in a way that is easy to analyse, as viewed in Figures 4.7, 4.9 and 4.11, especially with the ITAE and IAE values. Figures 4.8, 4.10 and 4.12 are graphically represented to show the load disturbance of both areas in the isolated power system using 1% and 2% respectively. The results displayed are similar to the load disturbance in a single area. From the first overview of the graphical representation, the results can be easily seen where the penetration of RES affects the system negatively by providing high oscillations and making the system extremely non-linear in all the simulation outputs

When comparing the results in area 1, PID with RES has displayed higher overshoots than the rest of the controller configurations for the full 50 second runtime with an ITAE performance of 2.269. PID was shown to produce multiple larger oscillations in all three depictions and cannot overcome the fluctuations from the high penetration of RESs. Therefore, this type of controller is not suitable for these applications. The PID controller time response for single load demand change in Area 1, Area 2 and Tie-line exceeds 50 seconds run time and doesn't approach steady state conditions. The PID controller time response for Area 1, Area 2 and Tie-line exceeds 50 seconds run time and doesn't approach steady state conditions for the load change of 1% in Area 1 and load demand change of 2% in Area 2. However, comparing the Figure 4.11 and Figure 4.12 tie-line representations, Figure 4.12 showcases fewer oscillations with the inclusion of RES than no RES for 50 seconds.

The FOPID with RES is able to bring the system back to steady state in all graphical outputs. The results show that the FOPID with RES has a settling time for all 6 graphical outputs at 8 seconds. However, there is multiple oscillations for 8 seconds that are present and the overshoot and undershoot is high in all the outputs which differs greatly. The FOPID has displayed better performance than the PID controller with the inclusion of the additional fractional order parameters. Proof of this is shown in Table 4.3.

For comparison, the error is simulated as 0.06176 for FOPID with RES, and 4.057 for PID with RES. This can be confirmed by the second performance criteria in Table 4.5 with 0.02205 for FOPID with RES, and 0.1638 for PID with RES. The controller brings the system to normal conditions with a lower wavelength and quicker response time. There are still minimum oscillations present, but much less than the PID controller. The overshoot in area 2 is shown to be very high due to the 2% load disturbance present, which contributed to the negative display of results. In the graphs presented, the settling time has an average of 8 seconds for FOPID.

In Area 1, Area 2, and for tie-line deviations, the FT1-FOPID with RES have shown good results, with the least settling time at 3.5 seconds and returning to steady state, little to no oscillations, and minimum overshoot of these controllers. The FT2-FOPID with RES has a settling time of 3 seconds for Area 1 and Area 2 graphical outputs. The tie-line graphical outputs have a settling time of 1.5 seconds for both the load demand change simulations. The controllers, including fuzzy, do not exceed 0.015, as displayed in the stand-alone FOPID and PID controllers for the area of error using ITAE. The stand-alone FOPID controller does return to the initial state, but takes a long time, which is 8 seconds with the error of 0.02066 using ITAE. The FT2-FOPID has shown to have the best results using IAE with the least error of 0.001161 and returns the system to steady state below 3 seconds. Therefore, the response time and performance of the FT2-FOPID are far superior to the traditional frequency controllers and FT1 logic systems. It is still evident that the inclusion of the RES in both areas contributes to a highly non-linear system which negatively impacts the isolated power system as shown in Tables 4.4 and 4.5.

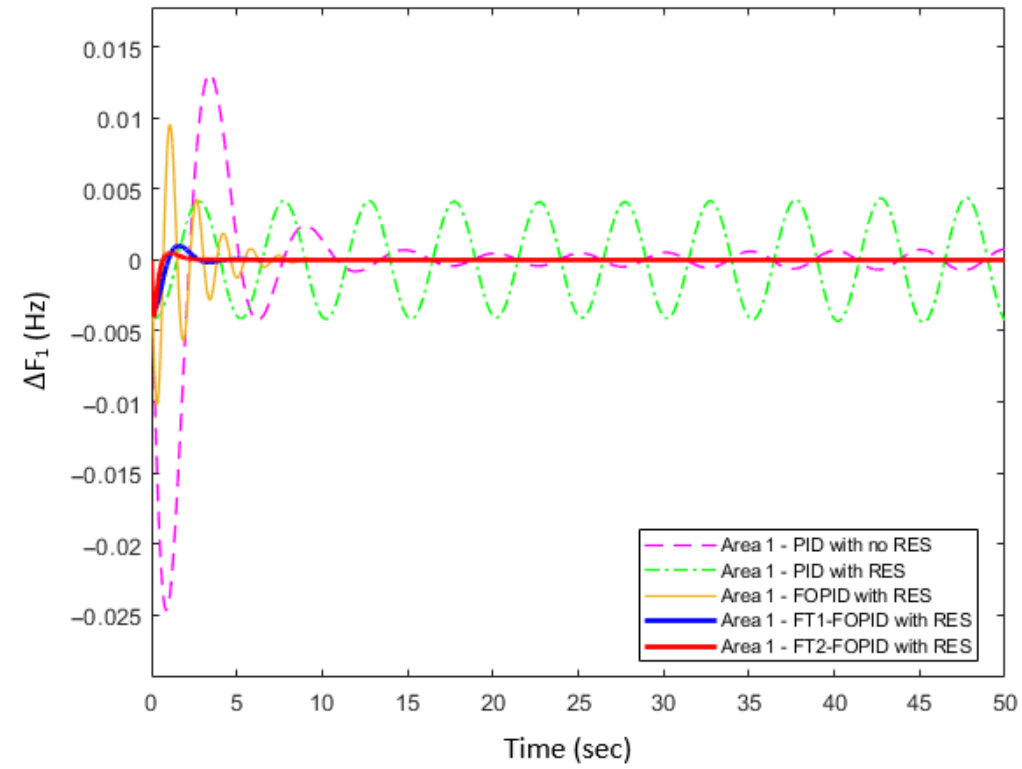

Figure 4.7: Results for 1% load alteration in area 1.

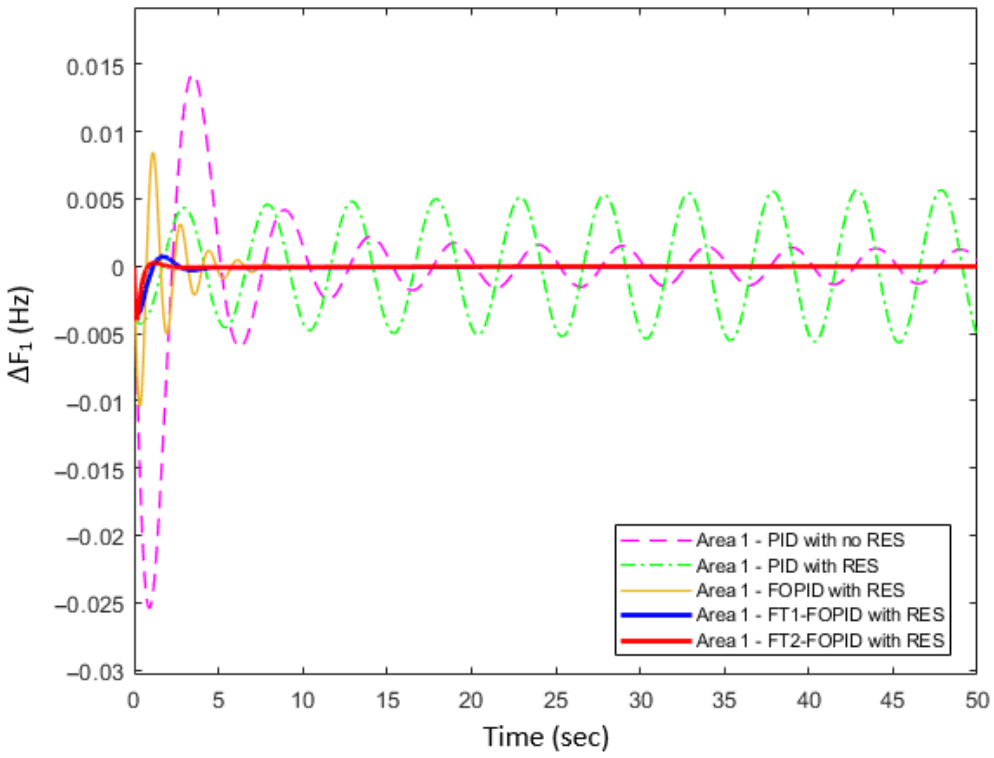

Figure 4.8: Results for 1% and 2% load alteration in area 1.

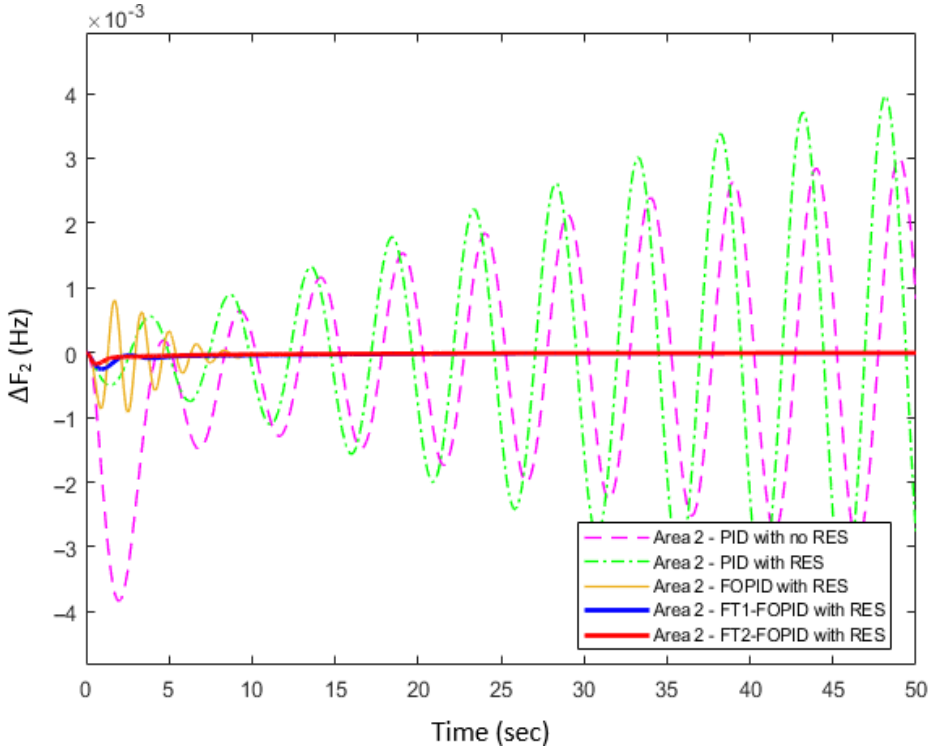

Figure 4.9: Results for 1% load alteration in area 2.

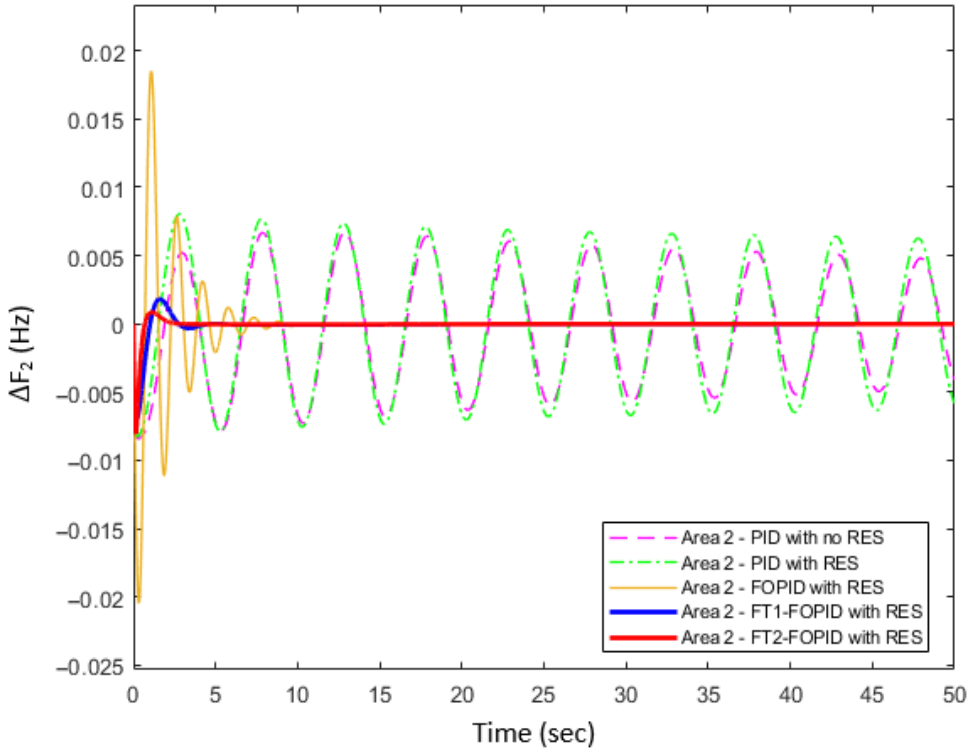

Figure 4.10: Results for 1% and 2% load alteration in area 2.

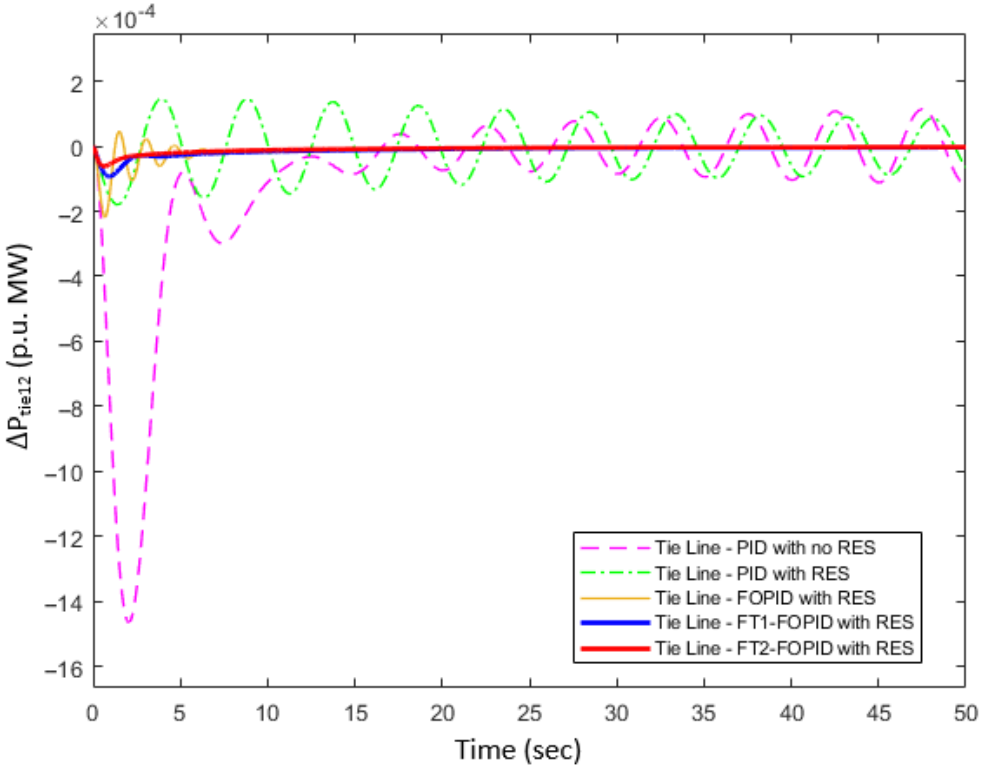

Figure 4.11: Results for 1% load alteration in tie-line.

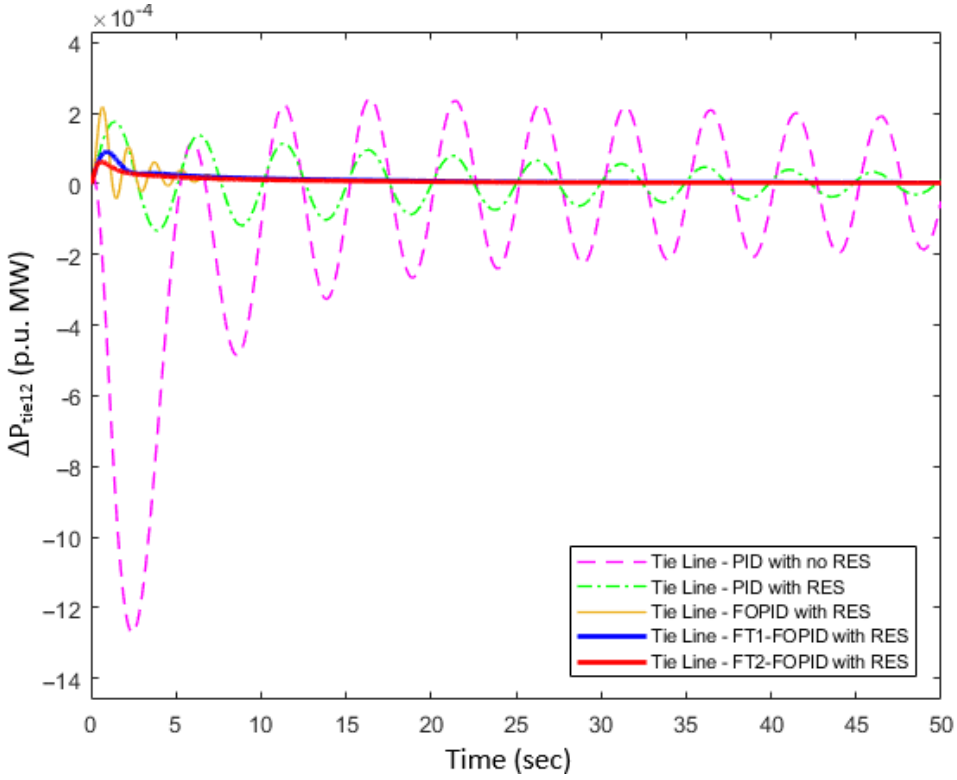

Figure 4.12: Results for 1% and 2% load alteration in tie-line.

The integration of fuzzy logic in the system has drastically improved the performance of the controllers, with the additional iterations of the logical system processes. With the fastest response time, least overshoot, best settling time, and no oscillations, the fuzzy logic controllers have the best performance with the least error for the two areas and tie-line region.

The FT2 system has a superior performance than type-1 which is evident in the depictions and the ITAE/IAE error values. With the NT reduction in type-2, the results are further fine-tuned to provide optimal performance. Wind and solar power have made the system highly non-linear due to the changing of wind rotor speeds and the irradiance from the solar panels, shading of panels, and inverters. The individual RES does have components and mechanisms in place to help curb these disturbances, but doesn't fully reduce them to zero. Therefore, the requirement for a secondary controller is required for additional assistance to mitigate these disturbances. Even though RES provides clean and renewable energy to the system, the higher the RES capacity, the greater the control is required for interconnected systems to work together.

From all the results displayed, the FT2-FOPID has the greatest performance of the rest of the controllers, with a slightly better edge than the FT1, which does not exceed ±0.005 Hz and has a 1 second less settling time than FT1. The error between the FT1 and FT2 has a difference of approximately 0.02 for change in demand for area 1 and area 2. The results illustrated on the above graph, and ITAE/IAE values, clearly show that RES creates disturbances when coupled with the isolated power system.

With the introduction of PID, the results had some control, but didn't come to steady-state conditions. FOPID with RES was shown to provide better results than PID with or without RES, therefore FOPID was used as the coupling controller for the fuzzy logic systems. The FT2-FOPID has proven itself to have lower overshoot and almost non-existent oscillations present. Even with the penetration of RES, the FT2 controller can handle the non-linearity which could harm the isolated power system. The applications of artificial intelligence can assist with control methods and solve unprecedented causes. With more processes being introduced, the controller can obtain better outputs and help the isolated power system overcome the disturbances as soon as possible.

4.3 Isolated Two Area Thermal Power System with PHEVs and RESs

The interconnected system was simulated on MATLAB/Simulink for the outcome and results of the isolated power system, without any errors occurring. The isolated power system consists of a solar-powered system, a wind-powered system, and a PHEV aggregator in each area. Both areas were controlled by a NNPC which predicts future possibilities when trained at 50 iterations to produce the best possible outcome. The system was then run for a time period of 50 seconds for change in load demand in area 1 to give results presented in Figures 4.13, 4.15 and 4.17. The system was run for a second time, but with a change in load demand in both areas, shown in Figures 4.14, 4.16 and 4.18. This was done to compare reasons for the performance of the controllers. The performance criterion is used for a clear view and interpretation of the results.

Table 4.6: Performance criterion results obtained for NNPC for demand change of 1% in area 1.

Controllers	**Performance Criterion**	**Isolated Two Area Power System**
Fractional Order PID	ISE	6.081×10^{-6}
	IAE	0.00506
	ITSE	-0.002587
	ITAE	0.01547
Interval Fuzzy Type-2	ISE	4.279×10^{-7}
	IAE	0.001187
	ITSE	-0.006353
	ITAE	0.007312
Neutral Network Predictive Controller	ISE	3.398×10^{-7}
	IAE	0.001086
	ITSE	-0.005285

Controllers	Performance Criterion	Isolated Two Area Power System
	ITAE	0.006013

Table 4.7: Performance criterion results obtained for NNPC for demand change of 1% in area 1, and 2% in area 2.

Controllers	Performance Criterion	Isolated Two Area Power System
Fractional Order PID	ISE	7.377×10^{-5}
	IAE	0.01483
	ITSE	-0.01807
	ITAE	0.04482
Interval Fuzzy Type-2	ISE	4.034×10^{-6}
	IAE	0.003609
	ITSE	-0.01939
	ITAE	0.02222
Neutral Network Predictive Controller	ISE	3.106×10^{-6}
	IAE	0.003095
	ITSE	-0.01541
	ITAE	0.01904

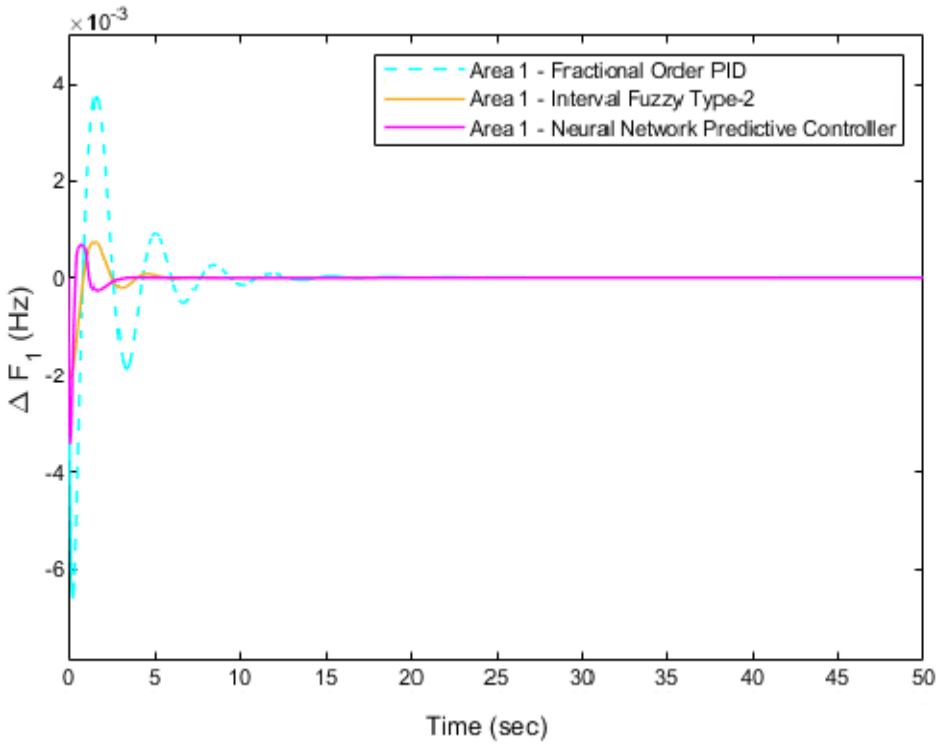

Figure 4.13: Area 1 output for a 1% demand change in area 1.

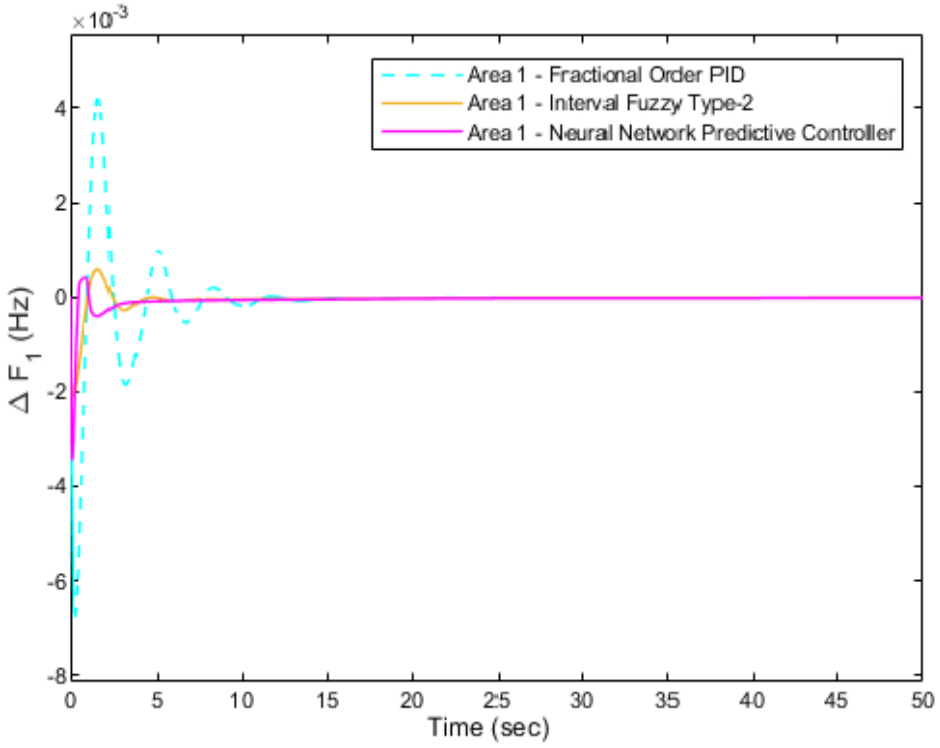

Figure 4.14: Area 1 output for a 1% demand change in area 1, and 2% demand change in area 2.

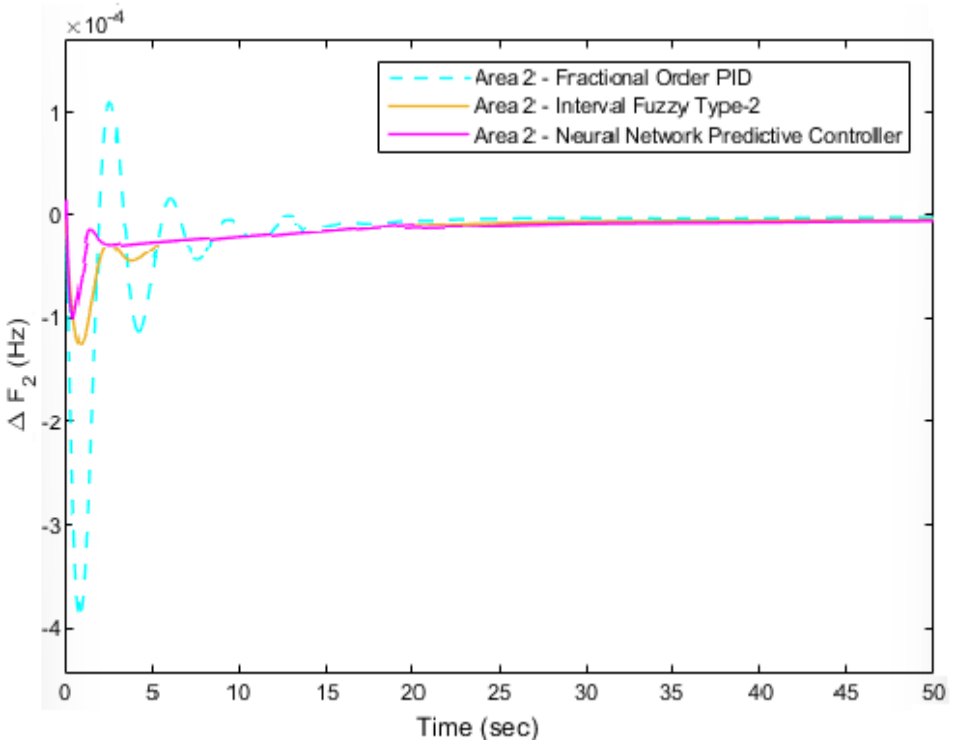

Figure 4.15: Area 2 output for a 1% demand change in area 1.

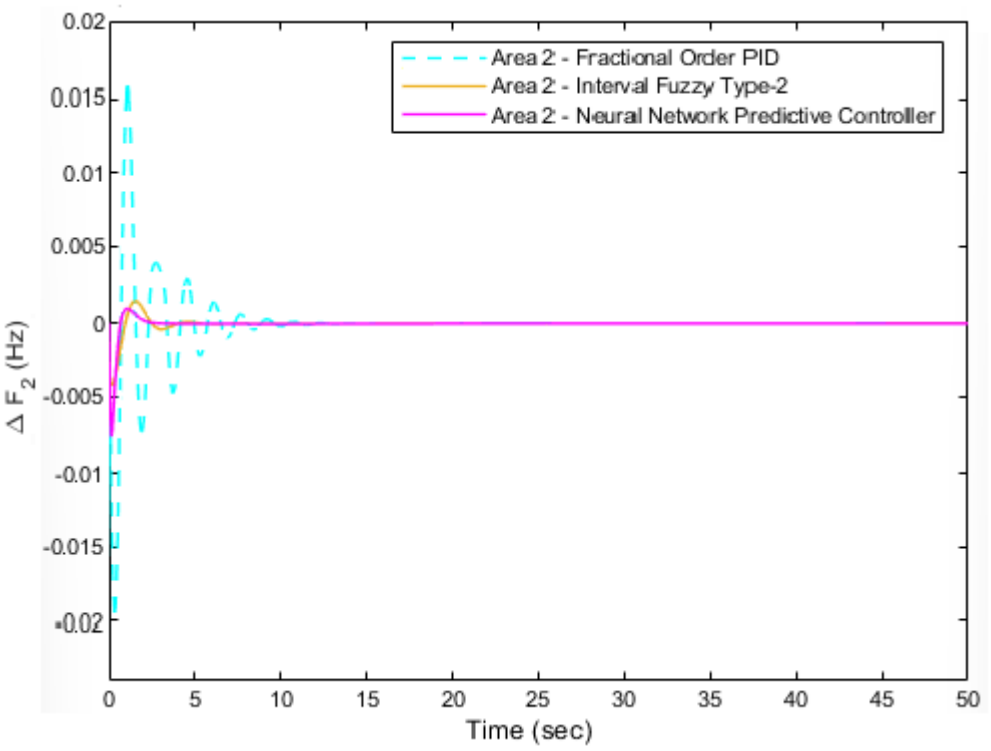

Figure 4.16: Area 2 output for a 1% demand change in area 1, and 2% demand change in area 2.

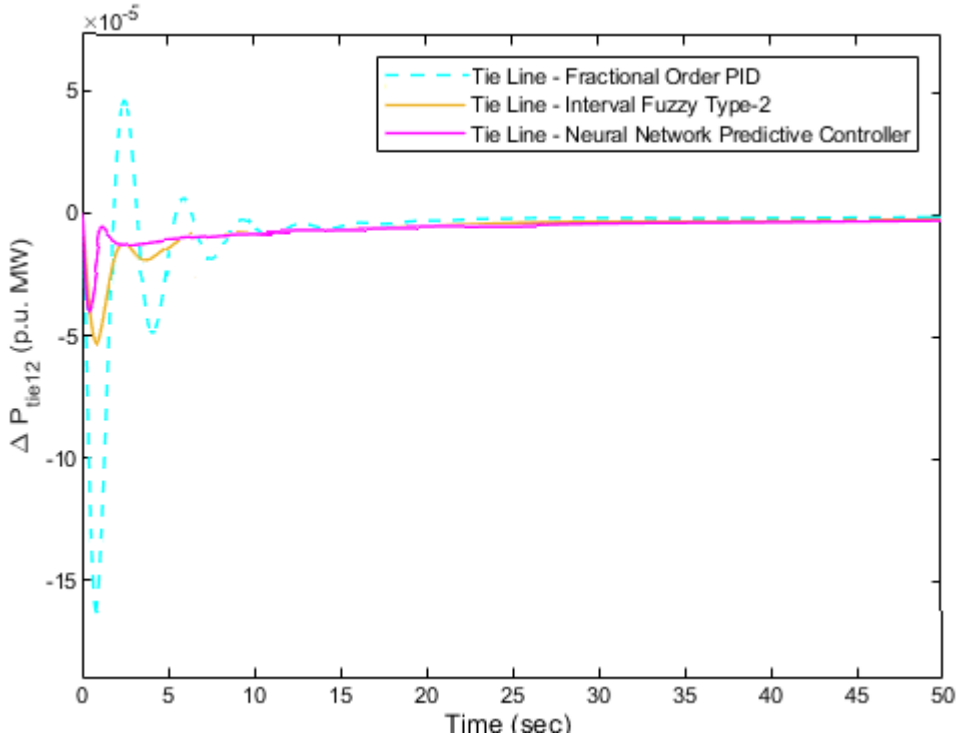

Figure 4.17: Tie-line output for a 1% demand change in area 1.

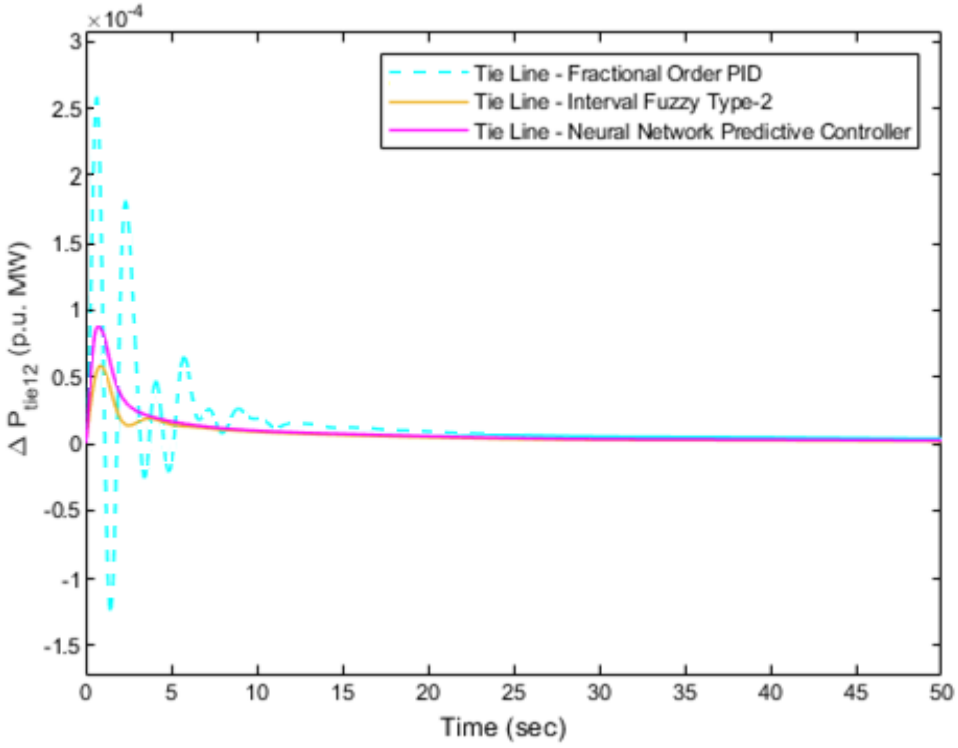

Figure 4.18: Tie-line output for a 1% demand change in area 1, and 2% demand change in area 2.

From the output illustrations shown above, for the load demand change in area 1 only, it is easily noticeable that the NNPC has superiority over the FOPID and interval FT2. This is similar for the load demand change in Area 1 and Area 2 simulations also. The reason for this can be explained in the performance criterion's values. The ISE shows that the overshoots to be the least for NNPC with 3.398×10^{-7} for single load demand change and 3.106×10^{-6} for a dual demand change when compared to the other controllers. That's approximately a 5% to 7% indifference from the controllers.

For area 1, the FOPID has a very high overshoot with 15 seconds of oscillation present that settles at 16 seconds. This is similar in area 2, but not in tie-line with a familiar behaviour but settling at 21 seconds. The interval FT2 presents a better output than the NNPC, with low oscillations presented in Figures 4.13, 4.15 and 4.17. The settling time is superior in area 1 but difficult to notice in area 2 and tie-line. According to the ITAE, the results for interval FT2 (0.007312) are better than FOPID (0.01547). The output is similar to the tie-line illustration. The error is reduced significantly but the settling time is similar. This is due to the complexity of the interconnected systems, which contributes to non-linearity and disturbances. The neural network has the fastest response time that reaches the steady state with minimum error and oscillations present. The peak overshoot is the lowest in Figures 4.13, 4.15 and 4.17. The settling time is similar to the FOPID.

For a load demand change in both areas, the oscillations for FOPID have displayed an increase in the results present in Figures 4.14, 4.16 and 4.18. The settling time ranges from 13 seconds in areas 1 and 2, and tie-line with 18 seconds, have the worst results compared to the other controllers used. The peak overshoot is the highest, for example as seen in Figure 4.17, with a value of 0.015 Hz. The ITSE result is shown to be 100% more than the NNPC. This makes the controller unsuitable for oscillation reduction.

The internal FT2 has presented much better results compared to the FOPID, with similar outcomes as the results in the simulation where there's load demand change for area 1 only. The IAE is very close, with values of 0.003609 for internal FT2 and 0.003095 for NNPC. The controller also shows better in results for tie-line error.

With the lowest overshoot, no oscillations present, fastest response and speedy settling time, the NNPC has the best output result overall. Area 1 displays the controller settling at 4 seconds, which shows the response of this controller. It is capable of tackling disturbance at a high-speed rate due to the predictive technology and analysis done through multiple iterations of future possibilities. Overall, this AI controller is superior to other controllers presented when it comes to steady-state stability and disturbances.

4.4 Chapter Summary

This chapter presents simulated results of three different scenarios utilising RES and PHEV configurations. The frequency is controlled via PID, FOPID, fuzzy logic and NNPC systems. The observations indicate that the interconnected system is improved using different control mechanisms in each scenario, while providing additional clean energy systems and disturbances. The RES has verified the fact that isolated power systems become highly non-linear due to their penetration, but can be brought to a steady state through systems on control. The PHEV has also demonstrated that it can assist with load variation in the isolated power systems. The conclusion and future improvements are discussed in the next chapter.

5. CONCLUSION AND RECOMMENDATIONS

5.1 Conclusion

This dissertation succeeded in an isolated two-area thermal power system integrated with RES and clean energy sources such as wind power, solar power and PHEV. Multiple arrangements and control strategies were used to assist with the frequency fluctuations of the interconnected systems, and a comparison was carried out to identify the best-performing controller.

For the first study involving PHEV, the inclusion of PHEVs into a conventional and isolated thermal power plant that is interconnected through an AC tie-line and controlled with FOPID, is modelled. To match the varying load demand in one or both areas with the generated power, multiple controllers - such as proportional, integral, and derivative controls - were used to establish the results of the isolated interconnected power system. Frequency studies have been done to verify the best controller design option through its performance. FOPID with PHEVs have shown to positively affect the control zones through stability enhancement, the least overshoot, and the provision of oscillation free for frequency and tie-line power deviations in LFC responses. Furthermore, PHEVs have enhanced the capacity of LFC which can act as a load or storage bank. This shows that incorporating them is possible through a centralised control system and an LFC which is utilised efficiently in the power grid, as and when required.

For the second study involving RES, the isolated thermal power system is interconnected via an AC tie-line to other areas with the isolated thermal power generation, resulting in an interconnected system. This system is controlled with the assistance of a FT2 logic controller, together with FOPID. Multiple configurations of controllers have been simulated, compared, and analysed to produce the most efficient output. The controller's main objective is to highlight the best performance in the overshoot, oscillations, and settling time of the frequency and power interchange over tie-lines, while experiencing a sudden change in load demand. The addition of DFIG-based wind turbines assists with the stability of the isolated power system, while the PV-based solar system introduces

fluctuations into the system due to its inverter, contributing to the slight disturbances even after the signal was filtered. The system, when interconnected with clean energy systems, can still become stable through the introduction of auxiliary control methods utilising type-2 fuzzy logic with FOPID, developed via PSO. The results guaranteed that the proposed design is well-suited for a renewable interlinked power system in comparison to results obtained via other control techniques. Further, the inclusion of non-linearities has shown a negative impact on all controllers' output, but still, type-2 fuzzy logic with FOPID is effective in providing the acceptable results for the isolated power system.

For the final study involving the RES and PHEVs, the scrutinised performance of the NNPC can be achieved for interconnected and isolated two-area power with RES and PHEV aggregators in each area. To confirm the effectiveness of the proposed controller, a comparison is done using FOPID, Interval FT2 and NNPC. The system performance is analysed with load disturbances in a single area, and then both areas. According to the outputs of the simulation, the system has a high penetration of RESs that contribute to multiple disturbances from changes in wind speeds, irradiance and load demand patterns. The system shows that RES contributes to non-linearity, therefore, load frequency controllers with optimisation are required. The NNPC contributes to a better overall result in terms of response and settling time, with better transient and steady-state responses.

5.2 Recommendation for Future Research

The need for clean, renewable energy with advanced control is vital for isolated power system stability. This study can be expanded for future research by considering the following suggestions:

1. Implementing a higher number of interconnected systems to increase the multi-area network and higher penetration of RES.
2. Further influential parameters that affect the current isolated power systems and RES can be introduced into the system to produce more accurate results.
3. Load demand change is highly variable creating random changes in isolated power systems, therefore a controller design for this variability is required to tackle random changes at any given point.

4. Design to consider load forecast of the isolated power systems and RES.
5. Further iterations of NNPC for more network training to achieve near-optimal control performance.
6. Possibility of future AI techniques that are more advanced and accurate for parameter development and non-linearity changes that can be integrated in the design model.

REFERENCES

[1] "Energy Sources: Renewables | Department: Energy | REPUBLIC OF SOUTH AFRICA." http://www.energy.gov.za/files/renewables_frame.html (accessed 14 July 2022).

[2] "List of power stations in South Africa - Wikipedia." https://en.wikipedia.org/wiki/List_of_power_stations_in_South_Africa (accessed 14 July 2022).

[3] "Top Countries in the Race to Net Zero Emissions - Net0." https://net0.com/blog/net-zero-countries (accessed 14 July 2022).

[4] D. Nichols and M. Brunell, *ALTI-ESS an Advanced Technology Power Plant for Grid Stabilization Applications*. 2011.

[5] N. Jaleeli, L. S. VanSlyck, D. N. Ewart, L. H. Fink, and A. G. Hoffmann, "Understanding automatic generation control," *IEEE Transactions on Power Systems,* vol. 7, no. 3, pp. 1106-1122, 1992, doi: 10.1109/59.207324.

[6] "Frequency Response Characteristics and Dynamic Performance," in *Robust Power System Frequency Control*, H. Bevrani Ed. Boston, MA: Springer US, 2009, pp. 1-24.

[7] E. Ela, M. Milligan, and B. Kirby, "Operating Reserves and Variable Generation," 01/01 2011, doi: 10.2172/1023095.

[8] A. F, C. I, G. I, and B. H. I, "Targets of Countries in Renewable Energy," in *2020 9th International Conference on Renewable Energy Research and Application (ICRERA)*, 27-30 Sept. 2020 2020, pp. 394-398, doi: 10.1109/ICRERA49962.2020.9242765.

[9] "UN Climate Change Conference (COP26) at the SEC – Glasgow 2021." https://ukcop26.org/ (accessed 14 July, 2022).

[10] M. S. Thopil, R. C. Bansal, L. Zhang, and G. Sharma, "A review of grid connected distributed generation using renewable energy sources in South Africa," *Energy Strategy Reviews,* vol. 21, pp. 88-97, 2018/08/01/ 2018, doi: https://doi.org/10.1016/j.esr.2018.05.001.

[11] F. Chishti, S. Murshid, and B. Singh, "Weak Grid Intertie WEGS With Hybrid Generalized Integrator for Power Quality Improvement," *IEEE Transactions on Industrial Electronics,* vol. 67, no. 2, pp. 1113-1123, 2020, doi: 10.1109/TIE.2019.2898598.

[12] W. Quincy and C. Liuchen, "An intelligent maximum power extraction algorithm for inverter-based variable speed wind turbine systems," *IEEE Transactions on Power Electronics,* vol. 19, no. 5, pp. 1242-1249, 2004, doi: 10.1109/TPEL.2004.833459.

[13] W. Wenjing, X. Jianing, S. Xin, L. Zhihui, Y. Yingqi, and W. Xinhe, "The research on correlation of electrical power system stability in high proportion wind power area," in *2021 IEEE International Conference on Power, Intelligent Computing and Systems (ICPICS)*, 29-31 July 2021 2021, pp. 563-567, doi: 10.1109/ICPICS52425.2021.9524200.

[14] J. M. Mauricio, A. Marano, A. Gomez-Exposito, and J. L. M. Ramos, "Frequency Regulation Contribution Through Variable-Speed Wind Energy Conversion Systems," *IEEE Transactions on Power Systems,* vol. 24, no. 1, pp. 173-180, 2009, doi: 10.1109/TPWRS.2008.2009398.

[15] C. Wu, X. P. Zhang, and M. Sterling, "Wind power generation variations and aggregations," *CSEE Journal of Power and Energy Systems,* vol. 8, no. 1, pp. 17-38, 2022, doi: 10.17775/CSEEJPES.2021.03070.

[16] C. Xing, X. Xi, X. He, C. Xiang, S. Li, and Z. Xu, "Research on Maximum Power Point Tracking Control of Wind-Solar Hybrid Generation System," in *2021 China International Conference on Electricity Distribution (CICED)*, 7-9 April 2021 2021, pp. 826-829, doi: 10.1109/CICED50259.2021.9556817.

[17] H. Wang *et al.*, "Evaluation Method of Wind Power Consumption Limitation in Power System with High Proportion of Wind Power," in *2021 IEEE 4th International Electrical and Energy Conference (CIEEC)*, 28-30 May 2021 2021, pp. 1-6, doi: 10.1109/CIEEC50170.2021.9510533.

[18] X. Ge, J. Qian, Y. Fu, W. J. Lee, and Y. Mi, "Transient Stability Evaluation Criterion of Multi-Wind Farms Integrated Power System," *IEEE Transactions on Power Systems,* vol. 37, no. 4, pp. 3137-3140, 2022, doi: 10.1109/TPWRS.2022.3156430.

[19] B. Spichartz, K. Günther, and C. Sourkounis, "New Stability Concept for Primary Controlled Variable Speed Wind Turbines Considering Wind Fluctuations and Power Smoothing," *IEEE Transactions on Industry Applications,* vol. 58, no. 2, pp. 2378-2388, 2022, doi: 10.1109/TIA.2022.3144650.

[20] G. J. P and M. B. J, "A Versatile Statcom for SSR Mitigation and Dynamic Reactive Power Management in DFIG Based Wind Farm Connected to Series Compensated Line," in *2020 IEEE International Power and Renewable Energy Conference*, 30 Oct.-1 Nov. 2020 2020, pp. 1-6, doi: 10.1109/IPRECON49514.2020.9315202.

[21] G. Sharma, K. R. Niazi, and Ibraheem, "Recurrent ANN based AGC of a two-area power system with DFIG based wind turbines considering asynchronous tie-lines," in *2014 International Conference on Advances in Engineering & Technology Research (ICAETR - 2014)*, 1-2 Aug. 2014 2014, pp. 1-5, doi: 10.1109/ICAETR.2014.7012881.

[22] J. Li *et al.*, "Stability Analysis of Wind Farm Connected to Hybrid HVDC Converter," in *2020 IEEE 9th International Power Electronics and Motion Control Conference (IPEMC2020-ECCE Asia)*, 29 Nov.-2 Dec. 2020 2020, pp. 3258-3262, doi: 10.1109/IPEMC-ECCEAsia48364.2020.9367833.

[23] Ibraheem, K. R. Niazi, and G. Sharma, "Study on Dynamic Participation of Wind Turbines in Automatic Generation Control of Power Systems," *Electric Power Components and Systems,* vol. 43, no. 1, pp. 44-55, 2015/01/02 2015, doi: 10.1080/15325008.2014.963266.

[24] W. Huang and W. Zhang, "Research on Distributed wind Power Reactive Voltage Coordinated Control Strategy Connected to Distribution Network," in *2021 4th International Conference on Energy, Electrical and Power Engineering (CEEPE)*, 23-25 April 2021 2021, pp. 529-534, doi: 10.1109/CEEPE51765.2021.9475820.

[25] A. J. Mahdi, W. H. Tang, and Q. H. Wu, "Derivation of a complete transfer function for a wind turbine generator system by experiments," in *2011 IEEE Power Engineering and Automation Conference*, 8-9 Sept. 2011 2011, vol. 1, pp. 35-38, doi: 10.1109/PEAM.2011.6134789.

[26] N. P. W. Strachan and D. Jovcic, "Improving Wind Power Quality using an Integrated Wind Energy Conversion and Storage System (WECSS)," in *2008 IEEE Power and Energy Society General Meeting - Conversion and Delivery of Electrical Energy in the 21st Century*, 20-24 July 2008 2008, pp. 1-8, doi: 10.1109/PES.2008.4596078.

[27] H. L. Jadhav, "Application of mechatronics in design and control of a quad-copter flying robot for aerial surveillance," *Excel Journal of Engineering Technology and Management Science,* vol. 1, no. 4, pp. 1-6, 2013.

[28] J. Driesen and K. Visscher, "Virtual synchronous generators," in *2008 IEEE Power and Energy Society General Meeting - Conversion and Delivery of Electrical Energy in the 21st Century*, 20-24 July 2008 2008, pp. 1-3, doi: 10.1109/PES.2008.4596800.

[29] Y. Chen, R. Hesse, D. Turschner, and H. Beck, "Improving the grid power quality using virtual synchronous machines," in *2011 International Conference on Power Engineering, Energy and Electrical Drives*, 11-13 May 2011 2011, pp. 1-6, doi: 10.1109/PowerEng.2011.6036498.

[30] W. Obaid and A. K. Hamid, "Grid-connected Hybrid Solar/Thermoelectric Power System with Hybrid INC/PSO/PO MPPT System in Sharjah, United Arab Emirates," in *2022 Advances in Science and Engineering Technology International Conferences (ASET)*, 21-24 Feb. 2022 2022, pp. 1-5, doi: 10.1109/ASET53988.2022.9734850.

[31] M. Badoni, A. Singh, S. Pandey, and B. Singh, "Fractional-Order Notch Filter for Grid-Connected Solar PV System With Power Quality Improvement," *IEEE Transactions on Industrial Electronics,* vol. 69, no. 1, pp. 429-439, 2022, doi: 10.1109/TIE.2021.3051585.

[32] M. S. Estrice, G. Sharma, K. T. Akindeji, and I. E. Davidson, "Frequency Regulation Studies of Interconnected PV Thermal Power System," in *2020 International SAUPEC/RobMech/PRASA Conference*, 29-31 Jan. 2020 2020, pp. 1-5, doi: 10.1109/SAUPEC/RobMech/PRASA48453.2020.9041043.

[33] B. K. F. Rodrigues, M. Gomes, x00C, M. O. Santanna, D. Barbosa, and L. Martinez, "Modelling and forecasting for solar irradiance from solarimetric station," *IEEE Latin America Transactions,* vol. 20, no. 2, pp. 250-258, 2022, doi: 10.1109/TLA.2022.9661464.

[34] C. Ghenai, F. Ahmad, M. A. Hussien, A. Merabet, and O. Rejeb, "Grid Connected Solar PV System for Green House Desalination Plant," in *2022 Advances in Science and Engineering Technology International Conferences (ASET)*, 21-24 Feb. 2022 2022, pp. 1-5, doi: 10.1109/ASET53988.2022.9734819.

[35] M. Estrice, G. Sharma, K. Akindeji, and I. E. Davidson, "Application of AI for Frequency Normalization of Solar PV-Thermal Electrical Power System," in *2020 International Conference on Artificial Intelligence, Big Data, Computing and Data Communication Systems (icABCD)*, 6-7 Aug. 2020 2020, pp. 1-4, doi: 10.1109/icABCD49160.2020.9183885.

[36] F. T. Tomy and R. Prakash, "Load frequency control of a two area hybrid system consisting of a grid connected PV system and thermal generator," *technology,* vol. 3, p. 4, 2014.

[37] F. Cao, J. Qiu, and Z. Jing, "Performance simulation and distribution strategy of solar and wind coupled power generation systems in Northwest China," in *2020 12th IEEE PES Asia-Pacific Power and Energy Engineering Conference (APPEEC)*, 20-23 Sept. 2020 2020, pp. 1-3, doi: 10.1109/APPEEC48164.2020.9220668.

[38] S. M. Abd-Elazim and E. S. Ali, "Load frequency controller design of a two-area system composing of PV grid and thermal generator via firefly algorithm," *Neural Computing and Applications,* vol. 30, no. 2, pp. 607-616, 2018/07/01 2018, doi: 10.1007/s00521-016-2668-y.

[39] Anuradha, A. S. Yadav, and S. Sinha, "Solar-Wind Based Hybrid Energy System: Modeling and Simulation," in *2021 4th International Conference on Recent Developments in Control, Automation & Power Engineering (RDCAPE)*, 7-8 Oct. 2021 2021, pp. 586-570, doi: 10.1109/RDCAPE52977.2021.9633590.

[40] X. Zhang, J. W. Spencer, and J. M. Guerrero, "Small-Signal Modeling of Digitally Controlled Grid-Connected Inverters With LCL Filters," *IEEE Transactions on Industrial Electronics,* vol. 60, no. 9, pp. 3752-3765, 2013, doi: 10.1109/TIE.2012.2204713.

[41] "South Africa to get $8.5 bln from U.S., EU and UK to speed up shift from coal." https://www.reuters.com/business/environment/us-eu-others-will-invest-speed-safricas-transition-clean-energy-biden-2021-11-02/ (accessed 14 July, 2022).
[42] M. E. Moeletsi and M. I. Tongwane, "Projected Direct Carbon Dioxide Emission Reductions as a Result of the Adoption of Electric Vehicles in Gauteng Province of South Africa," *Atmosphere,* vol. 11, no. 6, p. 591, 2020. [Online]. Available: https://www.mdpi.com/2073-4433/11/6/591.
[43] "Green Transport Strategy for South Africa: (2018-2050)." Transport.gov.za. https://www.transport.gov.za/documents/11623/89294/Green_Transport_Strategy_2018_2050_onlineversion.pdf/71e19f1d-259e-4c55-9b27-30db418f105a (accessed 14 July, 2022).
[44] M. Azeem, P. Kumar, A. Singhal, and S. Roy, "Performances of Hybrid Renewable Energy Based Electrical Charging Station," in *2022 International Conference for Advancement in Technology (ICONAT)*, 21-22 Jan. 2022 2022, pp. 1-5, doi: 10.1109/ICONAT53423.2022.9725855.
[45] S. Izadkhast, P. Garcia-Gonzalez, and P. Frías, "An Aggregate Model of Plug-In Electric Vehicles for Primary Frequency Control," *IEEE Transactions on Power Systems,* vol. 30, no. 3, pp. 1475-1482, 2015, doi: 10.1109/TPWRS.2014.2337373.
[46] W. Ran, L. Yifan, W. Ping, and D. Niyato, "Design of a V2G aggregator to optimize PHEV charging and frequency regulation control," in *2013 IEEE International Conference on Smart Grid Communications (SmartGridComm)*, 21-24 Oct. 2013 2013, pp. 127-132, doi: 10.1109/SmartGridComm.2013.6687945.
[47] A. Alobaidi, H. DesRoches, and M. Mehrtash, "Impact of Vehicle to Grid Technology on Distribution Grid with Two Power Line Filter Approaches," in *2021 IEEE Green Technologies Conference (GreenTech)*, 7-9 April 2021 2021, pp. 163-168, doi: 10.1109/GreenTech48523.2021.00035.
[48] D. Wu, N. Radhakrishnan, X. Ke, S. Huang, A. P. Reiman, and K. Kalsi, "Coordinated PEV Charging for Distribution System Management," 2019.
[49] E. Fouladi, H. R. Baghaee, M. Bagheri, and G. B. Gharehpetian, "A Charging Strategy for PHEVs Based on Maximum Employment of Renewable Energy Resources in Microgrid," in *2019 IEEE International Conference on Environment and Electrical Engineering and 2019 IEEE Industrial and Commercial Power Systems Europe (EEEIC / I&CPS Europe)*, 11-14 June 2019 2019, pp. 1-5, doi: 10.1109/EEEIC.2019.8783742.
[50] N. S. Koundinya, S. Vignesh, K. Narayanan, G. Sharma, and T. Senjyu, "Voltage Stability Analysis of Distribution Systems in the presence of Electric Vehicle Charging Stations with Uncoordinated Charging Scheme," in *2020 International Conference on Smart Grids and Energy Systems (SGES)*, 23-26 Nov. 2020 2020, pp. 303-308, doi: 10.1109/SGES51519.2020.00060.
[51] A. Annamraju and S. Nandiraju, "Coordinated control of conventional power sources and PHEVs using jaya algorithm optimized PID controller for frequency control of a renewable penetrated power system," *Protection and Control of Modern Power Systems,* vol. 4, no. 1, p. 28, 2019/12/26 2019, doi: 10.1186/s41601-019-0144-2.
[52] A. Hasankhani, S. M. Hakimi, M. Bodaghi, M. Shafie-Khah, G. J. Osório, and J. P. S. Catalão, "Day-Ahead Optimal Management of Plug-in Hybrid Electric Vehicles in Smart Homes Considering Uncertainties," in *2021 IEEE Madrid PowerTech*, 28 June-2 July 2021 2021, pp. 1-6, doi: 10.1109/PowerTech46648.2021.9494896.
[53] U. Cetinkaya, R. Bayindir, and S. Ayik, "Ancillary Services Using Battery Energy Systems and Demand Response," in *2021 9th International Conference on Smart Grid*

(icSmartGrid), 29 June-1 July 2021 2021, pp. 212-215, doi: 10.1109/icSmartGrid52357.2021.9551253.

[54] M. Akil, E. Dokur, and R. Bayindir, "Impact of Electric Vehicle Charging Profiles in Data-Driven Framework on Distribution Network," in *2021 9th International Conference on Smart Grid (icSmartGrid)*, 29 June-1 July 2021 2021, pp. 220-225, doi: 10.1109/icSmartGrid52357.2021.9551247.

[55] H. Jin, S. H. Nengroo, S. Lee, and D. Har, "Power Management of Microgrid Integrated with Electric Vehicles in Residential Parking Station," in *2021 10th International Conference on Renewable Energy Research and Application (ICRERA)*, 26-29 Sept. 2021 2021, pp. 65-70, doi: 10.1109/ICRERA52334.2021.9598765.

[56] M. Joshi, G. Sharma, and I. E. Davidson, "Load Frequency Control of Hydro Electric System using Application of Fuzzy with Particle Swarm Optimization Algorithm," in *2020 International Conference on Artificial Intelligence, Big Data, Computing and Data Communication Systems (icABCD)*, 6-7 Aug. 2020 2020, pp. 1-6, doi: 10.1109/icABCD49160.2020.9183829.

[57] A. Panwar, G. Sharma, I. Nasiruddin, and R. C. Bansal, "Frequency stabilization of hydro–hydro power system using hybrid bacteria foraging PSO with UPFC and HAE," *Electric Power Systems Research,* vol. 161, pp. 74-85, 2018/08/01/ 2018, doi: https://doi.org/10.1016/j.epsr.2018.03.027.

[58] S. Helm, I. Hauer, M. Wolter, C. Wenge, S. Balischewski, and P. Komarnicki, "Impact of unbalanced electric vehicle charging on low-voltage grids," in *2020 IEEE PES Innovative Smart Grid Technologies Europe (ISGT-Europe)*, 26-28 Oct. 2020 2020, pp. 665-669, doi: 10.1109/ISGT-Europe47291.2020.9248754.

[59] Y. Zhang, Y. Huang, Z. Chen, G. Li, and Y. Liu, "An Optimal Control Strategy for Plug-In Hybrid Electric Vehicles Based on Enhanced Model Predictive Control With Efficient Numerical Method," *IEEE Transactions on Transportation Electrification,* vol. 8, no. 2, pp. 2516-2530, 2022, doi: 10.1109/TTE.2022.3141191.

[60] S. Zhou, Z. Chen, D. Huang, and T. Lin, "Model Prediction and Rule Based Energy Management Strategy for a Plug-in Hybrid Electric Vehicle With Hybrid Energy Storage System," *IEEE Transactions on Power Electronics,* vol. 36, no. 5, pp. 5926-5940, 2021, doi: 10.1109/TPEL.2020.3028154.

[61] O. O. Olagbemi, P. Gómez, and R. T. Meyer, "Transient Analysis of Vehicle-to-Grid Systems Incorporating Plug-in Electric Vehicles," in *2021 56th International Universities Power Engineering Conference (UPEC)*, 31 Aug.-3 Sept. 2021 2021, pp. 1-6, doi: 10.1109/UPEC50034.2021.9548178.

[62] B. Das, P. K. Panigrahi, and C. K. Samant, "Impact Analysis of Plug-in Hybrid Electric Vehicle on Integration with Micro grid -A Review," in *2020 IEEE International Symposium on Sustainable Energy, Signal Processing and Cyber Security (iSSSC)*, 16-17 Dec. 2020 2020, pp. 1-5, doi: 10.1109/iSSSC50941.2020.9358824.

[63] G. Huang, H. Ma, X. Chen, B. Zhang, C. Liu, and J. Zhang, "Research on the optimal coordinated control strategy of 'source-grid-load-storage' including electric vehicle and distributed power supply," in *2020 IEEE International Conference on Artificial Intelligence and Information Systems (ICAIIS)*, 20-22 March 2020 2020, pp. 505-507, doi: 10.1109/ICAIIS49377.2020.9194707.

[64] H. Turker, "Optimal Charging of Plug-in Electric Vehicle (PEV) in Residential Area," in *2018 IEEE Transportation Electrification Conference and Expo (ITEC)*, 13-15 June 2018 2018, pp. 243-247, doi: 10.1109/ITEC.2018.8450125.

[65] S. S. Ravi and M. Aziz, "Utilization of Electric Vehicles for Vehicle-to-Grid Services: Progress and Perspectives," *Energies,* vol. 15, no. 2, p. 589, 2022. [Online]. Available: https://www.mdpi.com/1996-1073/15/2/589.

[66] Y. Yang, C. Qin, Y. Zeng, and C. Wang, "Optimal Coordinated Bidding Strategy of Wind and Solar System with Energy Storage in Day-ahead Market," *Journal of Modern Power Systems and Clean Energy,* vol. 10, no. 1, pp. 192-203, 2022, doi: 10.35833/MPCE.2020.000037.

[67] K. E. Årzén, M. Johansson, and R. Babuška, "Fuzzy Control Versus Conventional Control," in *Fuzzy Algorithms for Control*, H. B. Verbruggen, H. J. Zimmermann, and R. Babuška Eds. Dordrecht: Springer Netherlands, 1999, pp. 59-81.

[68] S. Vadi, F. B. Gurbuz, S. Sagiroglu, and R. Bayindir, "Optimization of PI Based Buck-Boost Converter by Particle Swarm Optimization Algorithm," in *2021 9th International Conference on Smart Grid (icSmartGrid)*, 29 June-1 July 2021 2021, pp. 295-301, doi: 10.1109/icSmartGrid52357.2021.9551229.

[69] M. A. El-Dabah, S. Kamel, M. Khamies, H. Shahinzadeh, and G. B. Gharehpetian, "Artificial Gorilla Troops Optimizer for Optimum Tuning of TID Based Power System Stabilizer," in *2022 9th Iranian Joint Congress on Fuzzy and Intelligent Systems (CFIS)*, 2-4 March 2022 2022, pp. 1-5, doi: 10.1109/CFIS54774.2022.9756463.

[70] J. Z. Shi, "A Fractional Order General Type-2 Fuzzy PID Controller Design Algorithm," *IEEE Access,* vol. 8, pp. 52151-52172, 2020, doi: 10.1109/ACCESS.2020.2980686.

[71] M. O. A. Kader, K. T. Akindeji, and G. Sharma, "A Novel Solution for Solving the Frequency Regulation Problem of Renewable Interlinked Power System Using Fusion of AI," *Energies,* vol. 15, no. 9, p. 3376, 2022. [Online]. Available: https://www.mdpi.com/1996-1073/15/9/3376.

[72] K. Saurabh, N. K. Gupta, and A. K. Singh, "Fractional Order Controller Design for Load Frequency Control of Single Area and Two Area System," in *2020 7th International Conference on Signal Processing and Integrated Networks (SPIN)*, 27-28 Feb. 2020 2020, pp. 531-536, doi: 10.1109/SPIN48934.2020.9070993.

[73] S. Sondhi and Y. V. Hote, "Fractional order PID controller for load frequency control," *Energy Conversion and Management,* vol. 85, pp. 343-353, 2014/09/01/ 2014, doi: https://doi.org/10.1016/j.enconman.2014.05.091.

[74] S. S. Pradhan, R. Pradhan, and B. Subudhi, "An Optimal Fractional-Order-Proportional-Integral Controller For a Grid-Tied Photovoltaic System," in *2021 International Symposium of Asian Control Association on Intelligent Robotics and Industrial Automation (IRIA)*, 20-22 Sept. 2021 2021, pp. 166-171, doi: 10.1109/IRIA53009.2021.9588694.

[75] C. Singh and P. K. Padhy, "Fractional Order Controller Design for interconnected Power System using BAT optimization Algorithm," in *2022 Second International Conference on Artificial Intelligence and Smart Energy (ICAIS)*, 23-25 Feb. 2022 2022, pp. 1634-1639, doi: 10.1109/ICAIS53314.2022.9743115.

[76] A. D. Shakibjoo, M. Moradzadeh, S. U. Din, A. Mohammadzadeh, A. H. Mosavi, and L. Vandevelde, "Optimized Type-2 Fuzzy Frequency Control for Multi-Area Power Systems," *IEEE Access,* vol. 10, pp. 6989-7002, 2022, doi: 10.1109/ACCESS.2021.3139259.

[77] K. Sabahi and M. Tavan, "T2FPID Load Frequency Control for a two-area Power System Considering Input Delay," in *2020 28th Iranian Conference on Electrical Engineering (ICEE)*, 4-6 Aug. 2020 2020, pp. 1-5, doi: 10.1109/ICEE50131.2020.9260608.

[78] O. Castillo and P. Melin, "A review on interval type-2 fuzzy logic applications in intelligent control," *Information Sciences,* vol. 279, pp. 615-631, 2014/09/20/ 2014, doi: https://doi.org/10.1016/j.ins.2014.04.015.

[79] İ. Kocaarslan and E. Çam, "Fuzzy logic controller in interconnected electrical power systems for load-frequency control," *International Journal of Electrical Power & Energy Systems,* vol. 27, no. 8, pp. 542-549, 2005/10/01/ 2005, doi: https://doi.org/10.1016/j.ijepes.2005.06.003.

[80] D. Rasi and S. N. Deepa, "Energy optimization of internet of things in wireless sensor network models using type-2 fuzzy neural systems," *International Journal of Communication Systems,* vol. 34, no. 17, p. e4967, 2021, doi: https://doi.org/10.1002/dac.4967.

[81] G. K. I. Mann, H. Bao-Gang, and R. G. Gosine, "Analysis of direct action fuzzy PID controller structures," *IEEE Transactions on Systems, Man, and Cybernetics, Part B (Cybernetics),* vol. 29, no. 3, pp. 371-388, 1999, doi: 10.1109/3477.764871.

[82] H. Bao-Gang, G. K. I. Mann, and R. G. Gosine, "A systematic study of fuzzy PID controllers-function-based evaluation approach," *IEEE Transactions on Fuzzy Systems,* vol. 9, no. 5, pp. 699-712, 2001, doi: 10.1109/91.963756.

[83] P. Bhatt, S. P. Ghoshal, and R. Roy, "Coordinated control of TCPS and SMES for frequency regulation of interconnected restructured power systems with dynamic participation from DFIG based wind farm," *Renewable Energy,* vol. 40, no. 1, pp. 40-50, 2012/04/01/ 2012, doi: https://doi.org/10.1016/j.renene.2011.08.035.

[84] I. Nasiruddin, G. Sharma, K. R. Niazi, and R. C. Bansal, "Non-linear recurrent ANN-based LFC design considering the new structures of Q matrix," *IET Generation, Transmission & Distribution,* vol. 11, no. 11, pp. 2862-2870, 2017, doi: https://doi.org/10.1049/iet-gtd.2017.0003.

[85] D. S. Sarali, V. A. I. Selvi, and K. Pandiyan, "An Improved Design for Neural-Network-Based Model Predictive Control of Three-Phase Inverters," in *2019 IEEE International Conference on Clean Energy and Energy Efficient Electronics Circuit for Sustainable Development (INCCES)*, 18-20 Dec. 2019 2019, pp. 1-5, doi: 10.1109/INCCES47820.2019.9167697.

[86] R. V. Yohanandhan and L. Srinivasan, "Decentralized Wide-Area Neural Network Predictive Damping Controller for a Large-scale Power System," in *2018 IEEE International Conference on Power Electronics, Drives and Energy Systems (PEDES)*, 18-21 Dec. 2018 2018, pp. 1-6, doi: 10.1109/PEDES.2018.8707660.

[87] Y. Wang, S. Wei, W. Yang, and Y. Chai, "Construction of offline predictive controller for wind farm based on CNN-GRNN," in *2021 CAA Symposium on Fault Detection, Supervision, and Safety for Technical Processes (SAFEPROCESS)*, 17-18 Dec. 2021 2021, pp. 1-6, doi: 10.1109/SAFEPROCESS52771.2021.9693547.

[88] D. Wang *et al.*, "Model Predictive Control Using Artificial Neural Network for Power Converters," *IEEE Transactions on Industrial Electronics,* vol. 69, no. 4, pp. 3689-3699, 2022, doi: 10.1109/TIE.2021.3076721.

[89] H. S. Khan, I. S. Mohamed, K. Kauhaniemi, and L. Liu, "Artificial Neural Network-Based Voltage Control of DC/DC Converter for DC Microgrid Applications," in *2021 6th IEEE Workshop on the Electronic Grid (eGRID)*, 8-10 Nov. 2021 2021, pp. 1-6, doi: 10.1109/eGRID52793.2021.9662132.

[90] R. Mohamed, B. Boudy, and H. A. Gabbar, "Fractional PID Controller Tuning Using Krill Herd for Renewable Power Systems Control," in *2021 IEEE 9th International Conference on Smart Energy Grid Engineering (SEGE)*, 11-13 Aug. 2021 2021, pp. 153-157, doi: 10.1109/SEGE52446.2021.9534982.

[91] M. Shouran and A. M. Alsseid, "Cascade of Fractional Order PID based PSO Algorithm for LFC in Two-Area Power System," in *2021 3rd International Conference on Electronics Representation and Algorithm (ICERA)*, 29-30 July 2021 2021, pp. 1-6, doi: 10.1109/ICERA53111.2021.9538646.

[92] P. Li, M. Zheng, D. Zhong, Y. Zheng, and G. Zhang, "Design of Fractional Order Controller for Microgrid Based on Model Analysis," in *2021 40th Chinese Control Conference (CCC)*, 26-28 July 2021 2021, pp. 52-57, doi: 10.23919/CCC52363.2021.9550290.
[93] "Solar GIS Resource Maps and GIS Data." https://solargis.com/maps-and-gis-data/overview (accessed 14 July, 2022).
[94] "Meteoblue." https://www.meteoblue.com/en/weather/week/south-africa_south-africa_8335359 (accessed 14 July, 2022).

APPENDIX

Appendix A: System Parameters

No.	Symbols	Name of parameter/constant
1	ΔP_{G_1}	Power of Governor 1
2	ΔP_{G_2}	Power of Governor 2
3	ΔP_{T_1}	Power of Turbine 1
4	ΔP_{T_2}	Power of Turbine 2
5	$\Delta P_{Tie_{12}}$	Power of Tie-line
6	ΔP_{PHEV_1}	Power of Plug in Hybrid Electric Vehicles Aggregator 1
7	ΔP_{PHEV_2}	Power of Plug in Hybrid Electric Vehicles Aggregator 2
8	Δf_1	Frequency in Area 1
9	Δf_2	Frequency in Area 2
10	$\frac{2\pi T_{12}}{s}$	Synchronizing Coefficient
11	$\frac{K_{G_1}}{1+sT_{G_1}}$	Generator Transfer Function 1
12	$\frac{K_{G_2}}{1+sT_{G_2}}$	Generator Transfer Function 2
13	$\frac{1+sK_{T_1}T_{T_1}}{1+sT_{T_1}}$	Reheat Turbine Transfer Function 1
14	$\frac{1+sK_{T_2}T_{T_2}}{1+sT_{T_2}}$	Reheat Turbine Transfer Function 2
15	$\frac{K_{P_2}}{1+sT_{P_2}}$	Generator Transfer Function 1
16	$\frac{K_{P_2}}{1+sT_{P_2}}$	Generator Transfer Function 2
17	β_1	Bias Coefficient 1
18	β_2	Bias Coefficient 2
19	a_{12}	Area Size Ratio Coefficient
20	ΔP_{SF}	Power from Solar Farm 1
21	ΔP_{SF_2}	Power from Solar Farm 2
22	ΔP_{WF_1}	Power from Wind Farm 1
23	ΔP_{WF_2}	Power from Wind Farm 2
24	ΔP_{D_2}	Change in Demand in Area 1

25	ΔP_{D_2}	Change in Demand in Area 2